ARCHIVES OF ACOUSTICS
5, 2, 125-142 (1980)

LONG-TIME SPECTRA OF RADIO BROADCAST PROGRAMME SIGNALS*

DÉNES HUSZTY

Elektroakustikai Gyár, Budapest, Hungary

Long-time spectra of signals of different radio broadcast programmes have been measured using the method of sample superposition (superposing signals of statistically independent sections of programme signals, recorded on tape, interpreted by ensembles with instruments of similar character). Spectra of signals of different ensemble groups (set of ensembles of equal composition of interpreters), having equal probabilities of occurrences, are calculated. Using programme policy statistics of three different transmitted programmes, the probabilities of occurrence of different ensemble classes (sets of ensembles, composed according to a rule) are calculated. Using these probabilities, the long-time-weighted spectra of the signals of three different radio programmes and the averages of these spectra are computed. The values are only slightly dependent on programme policy. A definition of the spectrally equivalent programme signal and a network for forming it are given.

Introduction

The original aim of this work was to collect data published in the literature in order to construct a network with the aid of which it would be possible to simulate adequately the spectral properties of a long-time-average radio broadcast programme signal. Collecting the data, we found that there exists a considerable amount of information concerning speech sounds, see e.g. [1]-[8], and also concerning musical sounds, see e.g. [2], [9], [10]-[17], but the data are insufficient for defining an artificial signal which has a power spectral density similar to that of a long-time-averaged broadcast programme signal. We have therefore conducted some work to obtain new data. This paper gives only a brief introduction to the problem and some of the results achieved; a more comprehensive review will appear elsewhere.

---

* Presented March 02. 1976, at the 53rd Convention of the Audio Engineering Society, Zurich, Switzerland.

The understanding of long-time-averaged spectra

It is evident that short-time statistical properties of the programme signal depend mainly on two things:

(a) The kind of signal that is transmitted at the moment of the measurement (e.g. speech or different music pieces etc.).

(b) The kind of interpreters that are working together during the performance (e.g. soloists with their given instruments or a symphonic orchestra, etc.); more shortly: what is being played by whom. Therefore if meaningful results of the short-time-statistical properties of the programme signal are to be obtained, knowledge of this data is also needed.

In the case of the long-time-spectra of the programme signals there is an additional problem: it is clear that these depend more or less on the programme policy of the broadcasting institution: a transmitted programme consisting of serious music and another consisting of popular music, must have very clearly different spectral properties. Thus if we need a realistic picture of the long-time spectral properties of an "average" radio broadcast programme containing mixed programme items, measurements must be made over a time interval long enough to ensure that different typical kinds of signals, generated by different, typical kinds of interpreters occur with typical frequencies.

It is not difficult to see that it is practically impossible to make such measurements because the time interval needed would be too long. We have therefore chosen another way. Namely that if the spectral properties of typical kinds of signals generated by typical kinds of interpreters are known, and if the probabilities of occurrence of these signals over a long enough time are known then we can calculate the long-time-spectral properties of the programme signal. In other words: it is necessary to have an average over the programme signals generated by sound sources of typical interpreters interpreting typical kinds of programme items, weighted by the probabilities of occurrences of these interpretations. This has been done in three steps as follows.

The theoretical background of the method

In order to obtain meaningful results some general assumptions have been made for the signals measured [18]:

(a) The programme signals belonging to different programme items are sample functions of separable, weakly stationary stochastic processes having expected values equal to zero.

(b) These stochastic processes are completely independent and their power spectral density functions exist.

(c) These stochastic processes satisfy all the assumptions necessary to permit ergodicity of almost all of their first and second-order statistical properties, to be assumed.

(d) The duration of measurements of the sample functions is long enough to have a small statistical error but short enough to secure stationarity in the weak sense. (For probabilistic concepts see e.g. [19].) We assume that the programme signals considered fulfil all of these requirements.

We should emphasize that according to these assumptions we are considering the programme signal measurable over a long time, as a linear sum of sample functions of different stochastic processes, stationary in the weak sense and ergodic in their first and second-order properties. This means that we give, for example, to the speech waves of the different speakers, different sample functions, and these sample functions belong to different stochastic processes. The procedure used is the same for music, also. This point of view has a significance of a fundamental character and differs clearly from that used tacitly in the literature where for example speech, as a whole, has been considered as one stochastic process and the speech waves of individual speakers as sample functions of this process.

As a consequence of these assumptions it can be shown [18] that the sum of sample functions of equal length has the same first and second-order statistical properties (expected values, autocorrelation functions, powers, power spectral distributions) as a sample of a signal whose consecutive parts are the said sample functions added. This signal is then no other than the real programme signal having a total length that of the summands. Thus it does not matter whether the summing is performed mathematically or physically, by which we mean the simultaneous observation — measurement — of a set of sample functions of equal duration, belonging to different stochastic processes, i.e. belonging to different parts of programme signals of different programme items of equal length.

It is clear that each sample function has been generated by an ensemble, i.e. the nonempty set of interpreters coworking in generating the programme signal, corresponding to a given programme item. Consequently, each ensemble — which can be a single speaker or a large symphonic orchestra — has its typical sound generating instruments. These instruments are by no means identical but are similar in their sound generating properties as ensembles with the same composition of interpreters. We have thus defined an ensemble group as the set of ensembles having a nominally equal composition of interpreters. This "equality" cannot be seen too strictly: each symphonic orchestra is to be regarded belonging to the same ensemble group, in spite of a different composition in practice. If we now choose, for each ensemble of an ensemble group, different but typical programme material to be interpreted by their sound generating mechanisms, then the statistical properties of the simultaneously observed sample functions will be typical for the group.

Using this train of thought we can achieve data for each of the different ensemble groups. Now let us construct an upper level: we define a nonempty set of different ensemble groups as an ensemble class where the composition

of the class follows a rule. This rule cannot be similar to those of the groups; it is better if we define it more or less according to the programme statistics available. The concept, shown by Table I, seems to be self explanatory. The statistical properties of a given ensemble class can be now calculated using the above mentioned assumptions simply by adding the sample functions. It should be noted that additivity is valid only for the expected values, the autocorrelation functions and the spectral properties but by no means for, for example, the long-time-averaged peak factor of the programme signal, which can be only measured. Although there is a possibility of estimating the least upper limit.

Thereafter if we have the statistics of the occurrence of different items in the programme transmitted, characterising the programme policy of the broadcast institution, we can calculate the weighted averages of the data of each ensemble classe, where the weights are the probabilities of occurrence of each ensemble classe in the statistics, collected over a long enough time interval.

It should be mentioned that the simultaneous observation i.e. the measurement of a set of superposed sample functions using sounds from different speakers was originated intuitively by TARNÓCZY [6]. Probably because of the lack of a sufficient theoretical basis he was of the opinion that this method, called by him the "speech chorus method", can only be used for speech sounds [11]. It is however clear that it is by no means necessary to restrict this ingenious method, which may perhaps better be called the "method of sample superposition", to speech sounds alone.

Method of measurement

In order to produce the superposed samples, i.e. to construct the programme signal of an ensemble group, we have chosen, for each group, six different two-minute long samples of typical programme items recorded on studio tapes. These six samples were subsequently simultaneously copied onto a single tape, using six studio tape recorders and a studio mixing desk, as shown in Fig. 1*a*.

This sixfold record has been cut into four equal parts. After simultaneous copying of these parts the record contained the superposition of 24 samples of practically independent programme signals. This record of $T = 30$ s duration was regarded as the programme signal of the ensemble group considered. A value of $T = 30$ s was chosen for the length because musical phrases have approximately this length or less. The sound generated by this record is like a noise; it is not possible to hear any kind of melody.

The spectral properties of this record have been analysed for rms and peak power using setup shown in Fig. 1*b*, first over the whole audio frequency range

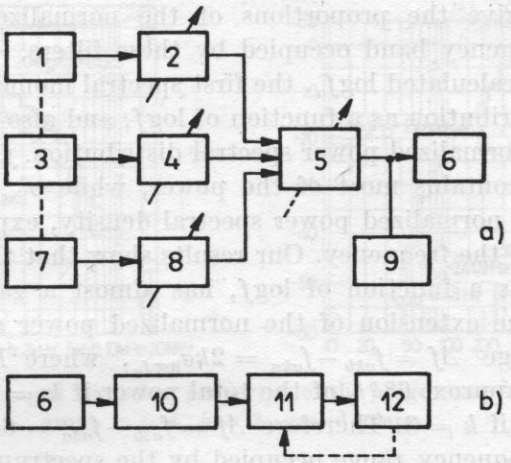

Fig. 1. a. Arrangement used for reconstructing the programme signal of an ensemble group. b. Arrangement used for measuring the programme signal of an ensemble group
1 – 1st tape recorder STM 200/b, *2* – 1st line amplifier, *3* – kth tape recorder STM 200/b, *4* – kth line amplifier *5* – summing amplifier, *6* – tape recorder STM/b (in a)) or STM 10 (in b)), *7* – 6th tape recorder STM 200/b, *8* – 6th line amplifier, *9* – programme level meter, *10* – input transformator B-Kj Tl 0001, *11* – 1/3 oct. filter B-Kj 2112, *12* – level recorder B-Kj 2305

and thereafter in 26 different 1/3 octave bands, beginning at 50 Hz. The level recorder has been used as an integrating instrument, with a 50 dB potentiometer using 50 dB potentiometer-range, and a 20 Hz lower limiting frequency setting. The writing speed was 2 mm/s. These settings corresponded to an effective averaging time of approx. 12 s [20].

Evaluation of the results

The results of the measurements have been evaluated as level differences referred to the long-time averaged rms voltage level of the unfiltered signal. The level of this has been chosen as the 0 dB reference level. In each case we have calculated $20 \log \bar{K}_p = \bar{L}_p - \bar{L}_e$, where $\bar{K}$ is the long-time-averaged peak factor and $\bar{L}_p$ is the long-time-averaged peak voltage level referred to $\bar{L}_e = 0$ dB. Then, using the measured results, we have evaluated the values of $\bar{L}_e(f_m)$, $\bar{L}_p(f_m)$ and $20 \log \bar{K}_p(f_m)$ where $f_m (m = 1, 2, \ldots, 26)$ are the mid-band frequencies of the 1/3 octave filters, beginning at $f_1 = 50$ Hz.

Using these data we have calculated the values $10 \log N_l[h(f_{ln})]$ and $10 \log N_h[n(f_{hn})]$. The former is essentially $N_l[n(f_{ln})]$ the normalized power spectral distribution, expressed in dB, as a function of the frequency $f_{ln} (n = 1, 2, \ldots, 26)$. The latter is then $10 \log \{1 - N_l[n(f_{ln})]\}$, also expressed in dB, as a function of the frequency $f_{hn} (n = 1, 2, \ldots, 26)$. Identifying f_{ln} and f_{hn} as the last and first mid-band frequencies respectively of a low pass or high pass filter, composed of 1/3 filters with ideal cut-off, $10 \log N_l[n(f_{ln})]$, and

$10 \log N_h[n(f_{hn})]$ give the proportions of the normalized power, expressed in dB, in the frequency band occupied by these filters.

We have also calculated $\log f_a$, the first spectral moment of the normalized power spectral distribution as a function of $\log f$, and also $\sigma^2_{\log f_a}$, the variance, belonging to this normalized power spectral distribution. f_a gives the frequency whose neighbour contains most of the power, while $\sigma^2_{\log f_a}$ characterizes the "peakiness" of the normalized power spectral density, expressed as a function of the logarithm of the frequency. Our results show that the normalized power spectral density, as a function of $\log f$, has almost a gaussian shape. Using this assumption the extension of the normalized power spectral density, i.e. the frequency range $\Delta f = f_{akb} - f_{aka} = 2k\sigma_{\log f_a}$, where k is a nonnegative number, contains approx. 68 % of the total power if $k = 1$, and approx. 99 % of the total power if $k = 3$. Therefore $\Delta f = f_{a3b} - f_{a3a} = 6\sigma_{\log f_a}$ gives approximately the full frequency range occupied by the spectrum of the programme signal considered. Thereafter we have calculated n_a, frequency-weighted average of the normalized power spectral density; small values give correspondingly peaked spectral densities as a function of $\log f$.

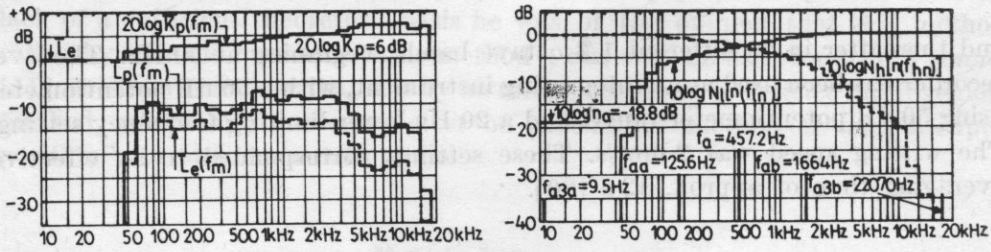

Fig. 2 a, b. Long-time-averaged statistical properties of the programme signal of the ensemble group $x = 3$, $y = 2$: pop group

Some results measured

In order to demonstrate some of the results achieved Figs. 2*a* and 2*b* show the long-time-averaged statistical properties of the ensemble group: a pop ensemble, $x = 3$, $y = 2$. This was one of the ensemble groups whose spectrum occupies the broadest frequency band. As Fig. 2*a* shows, $\bar{L}_e(f_m)$, the long-time-averaged rms level, shows only a variation of about 5 dB — as a function of f_m, the mid-band frequency of the 1/3 octave bands considered — over the range from 63 Hz to 3 kHz. Most of the power — indicated by Fig. 2*b* — lies near the first spectral moment $f_a = 457.2$ Hz. The frequency band occupied is very large: $\Delta f = f_{a3b} - f_{a3a} \approx 22$ kHz.

Figs. 3*a* and 3*b* show the results obtained for the ensemble group: grand piano, $x = 4$, $y = 3$. This has one of the most peaked spectra among the ensemble

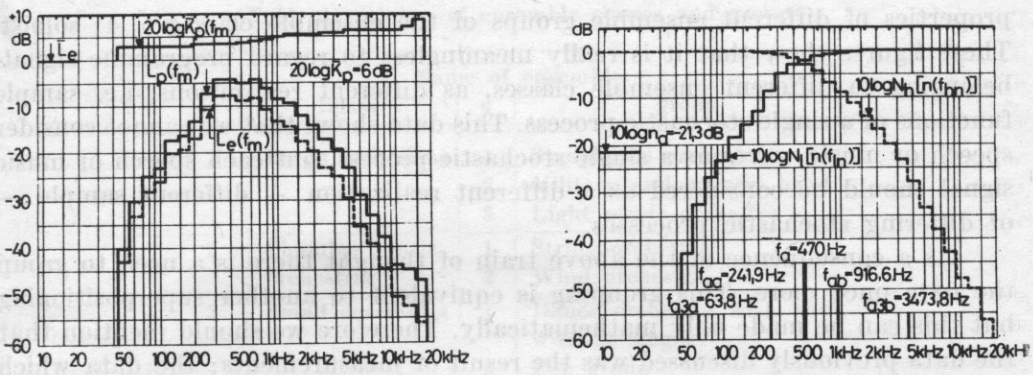

Fig. 3 a, b. Long-time-averaged statistical properties of the programme signal of the ensemble group $x = 4$, $y = 3$: grand piano

groups considered, as can be seen from Table I. The extension of the normalized power spectral density shown by Δf, $\Delta f = f_{a3b} - f_{a3a} \approx 3400$ Hz, is considerably narrower than that of the pop group.

The question arises whether or not the data achieved for a given group is really characteristic of the properties of the group considered? In some cases the measurements were repeated using other programme materials for composing the programme signal of the group. The results were quite similar: there being no more than 2 dB deviation in the levels obtained. This shows that the method of "sample superposition" is useful and adequate for obtaining characteristic results.

In order to show why broad spreadings in the results obtained for different ensemble groups exist, the reader is referred to see Figs. 4*a* and 4*b*, where $J[\cdot]$ denotes the interval occupied by the characteristics considered. We should mention that this large spreading has been caused mostly by the very different

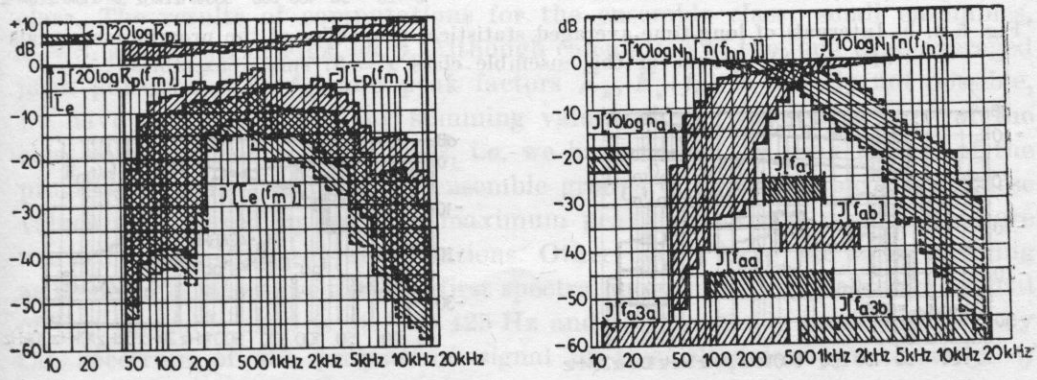

Fig. 4 a, b. Intervals of long-time-averaged statistical properties of the programme signals of all the ensemble groups considered (see Table 1)

properties of different ensemble groups of the ensemble class $x = 4$: soloist. These figures show that it is really meaningless to regard programme signals belonging to different ensemble classes, as different realizations, i.e. sample functions of a single stochastic process. This data shows that we cannot consider speech or music waves as a single stochastic process, but each speech or music signal should be considered as a different realization — different sample — of differing stochastic processes.

As a consequence of the above train of thought there is a need to group the data once more. This grouping is equivalent to another superpositioning but this can be made only mathematically. Therefore we should mention that the data previously discussed was the result of measurements; the data which will be shown subsequently is the result of computation.

Selected computed results

As a result of the assumptions made, we can calculate the programme signal of each ensemble class. The necessity for this can be seen in Figs. 5*a* and 5*b*, which show the intervals occupied by the different data obtained for the different ensemble groups $y = 1, 2, 3, 4$ of the ensemble class $x = 3$ (small

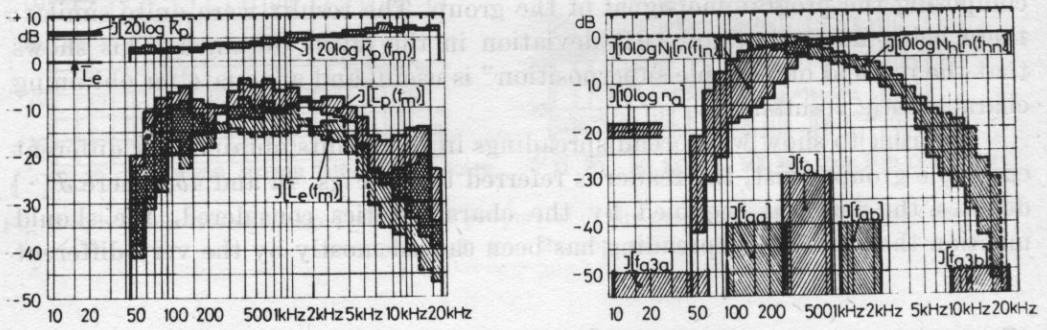

Fig. 5 a, b. Intervals of long-time-averaged statistical properties of the programme signals of ensemble groups of the ensemble class $x = 3$: small ensembles

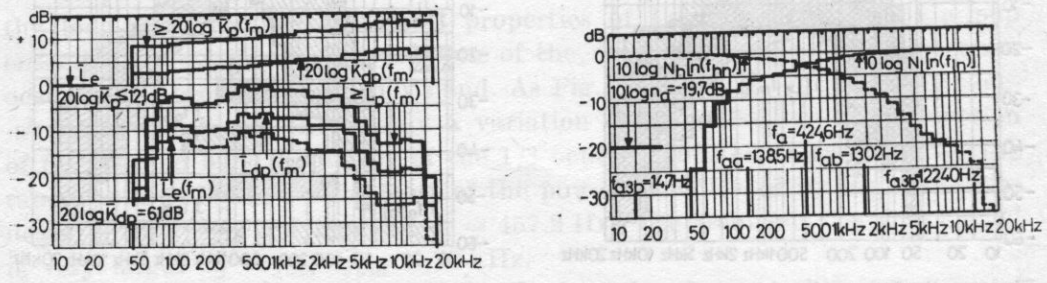

Fig. 6 a, b. Long-time-averaged statistical properties of the programme signal of the ensemble class $x = 3$: small ensembles

Table 1. Scheme of ensemble classes and groups

Name of ensemble			
x	class	y	group
1	Large orchestras	1	Symphonic orchestra
		2	Military and concert band
		3	Light music orchestra
2	Chamber music orchestras	1	String orchestra
		2	Wind orchestra
3	Small ensembles	1	Dance orchestra with and without singer
		2	Pop group
		3	Jazz ensemble
		4	Folk ensemble
4	Soloists	1	Violin
		2	Violoncello
		3	Grand piano
		4	Cemballon
		5	Organ
		6	Violin with grand piano
		7	Wind instr. with grand piano
		8	Singer with grand piano
5	Stage ensembles	1	Ensemble for opera
		2	Ensemble for operette
6	Mixed singing choirs		
7	Voices	1	Male voice
		2	Female voice
		3	Radio drama

ensembles, see Table 1). The data shown in these figures should be considered typical of the spreading of data for the ensemble groups of a given ensemble class. The results of computations for the ensemble class: small ensembles, $x = 3$, are shown in Figs. 6*a*, *b*. Although calculation of the long-time-averaged peak powers $\bar{L}_p$, $\bar{L}_p(f_m)$ and peak factors $\bar{K}_p$, $\bar{K}_p(f_m)$ is strictly not possible, we have calculated these by summing values of the different groups of the class considered on a linear basis, i.e. we have added the peak powers of the programme signals of different ensemble groups of the ensemble class. These values are indexed by *dp*. The maximum peak powers and peak factors are marked by $\geqslant$ before the abbreviations. Other marks have the same meaning as before. Fig. 6*b* shows that the first spectral moment of the programme signal of this ensemble class is at $f_a \approx 425$ Hz and the frequency band occupied by the spectrum of the programme signal of this class is approximately $\Delta f \approx 12.26$ Hz.

We have also calculated data belonging to each of the ensemble classes

of Table 1. The differences between the data from the ensemble classes were then considerably smaller than the data from different ensemble groups as a consequence of the averaging, but large enough to indicate that they are characteristic of the properties of the programme signal of the ensemble class considered.

The weighted programme signal

The next step was the collection of the statistical data on the occurrences of different programme items in different radio broadcast programmes. Data was found [21] for different quarters of different years, denoted by k. Naturally, this data had been originally collected for an other purpose, so that it was necessary to perform some transformation before using it. The method of transformation and the method of calculation of the probability ${}_xW_k$, of the occurrence of a given ensemble class in a given quarter of year k, are shown in Table 2. This validates our method of grouping ensemble groups into ensemble classes according to the classification in Table 1.

Table 2. Method of calculation of ${}_xW_k$, the probability of occurrence of different encemble classes in a given quarter of a year k

x	${}_xW_k$
1	(programme time of symphonic music + military or concert bands + light music + 1/3 of the presentation of popular education) · (full programme time)$^{-1}$
2	(programme time of chamber music + 1/3 of the presentation of popular education) · (full programme time)$^{-1}$
3	(programme time of dance music + pop music + jazz music + folk music + morning musical programmes) · (full programme time)$^{-1}$
4	(programme time of solos + songs) · (full programme time)$^{-1}$
5	(programme time of operas + operettas + parts of them + 1/3 of the presentation of popular education) · (full programme time)$^{-1}$
6	Mixed singing choirs (programme time of choruses + mass songs) × × (full programme time)$^{-1}$
7	$1-\sum_{x=1}^{6} {}_xW$

There were only two sorts of programmes which were somewhat outside our method of grouping, namely the presentation of popular education and morning musical programmes. However, the second dealt with music, played by large or chamber orchestras, or by some kind of stage ensembles, interconnected with some speech of much shorter duration. We have therefore divided this programme time into three equal parts and these have then been added to the programme times of the above mentioned ensemble classes. The morning musical programmes correspond in their contents — apart form the short periods of speech connecting the music — with those of the pieces interpreted by small ensembles.

In Hungary three different radio programmes are broadcast. Taking this in account we have collected data and have calculated the weighted long-time-spectral properties for each of these different radio broadcast programmes and also their averages. Fig. 7 shows the probability of occurrence of the diffe-

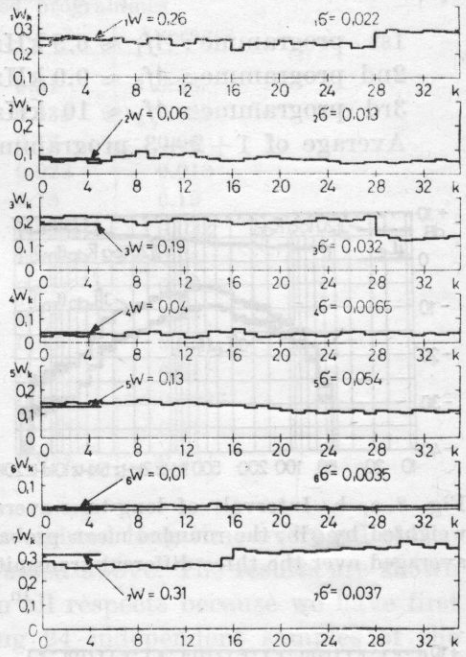

Fig. 7. Rounded probabilities of occurrences of different ensemble classes, ${}_xW_k$, as a function of the quarter year k, beginning at 1965. The data is the average from three different programmes. ${}_xW$ are averages over k and ${}_x\sigma$ are the standard deviations of the occurrences ${}_xW_k$, averaged over the three different programmes, of the ensemble class x

rent ensemble classes, ${}_xW_k$, $x = 1, \ldots, 7$, as a function of k, the index for a quarter of a year, beginnning at 1965. This data is the result of an averaging over the probabilities of occurrences of the three different programmes. Fig. 7 shows ${}_x\sigma$, the standard deviations of occurrence of each of the ensemble classes of these programmes, and time averaged data. It is clear that the probability of occurrence of different ensemble classes is quite uniform as a function of k, i.e. time, showing stability of the programme policy of the broadcast institution.

It is also interesting to analyse the mean values ${}_xW$ and standard deviations ${}_x\sigma$ of probability of occurrence of the different ensemble classes in the different transmitted programmes, as shown in Table III. The last column of the table gives the averages of the three different transmitted programmes, which are also shown in Fig. 7. The deviations between the mean probabilities ${}_xW$ obtained for the different programmes are not too severe.

Using these mean values, ${}_xW$, we have calculated the weighted averages of the programme signals of different ensemble classes, on a linear basis for each transmitted programme, called the programme signal of transmitted programme 1, 2, or 3, by adding the probability — weighted powers. The weights here physically correspond to power gains. It is interesting to note that in spite of the fact that the differences between the spectral values obtained for the three different programmes are not larger than 2 dB, as shown in Figs. 8*a*, 8*b*, there are considerable differences between the frequency ranges occupied by these three different programmes:

1st programme : $\Delta f_1 \approx 6.9$ kHz, $f_{a1} \approx 452$ Hz;
2nd programme : $\Delta f_2 \approx 9.0$ kHz, $f_{a2} \approx 470$ Hz;
3rd programme : $\Delta f_3 \approx 10$ kHz, $f_{a3} \approx 512$ Hz.
Average of 1+2+3 programmes : f_{mean} 9.2 kHz, $f_{a\text{mean}} \approx 477$ Hz.

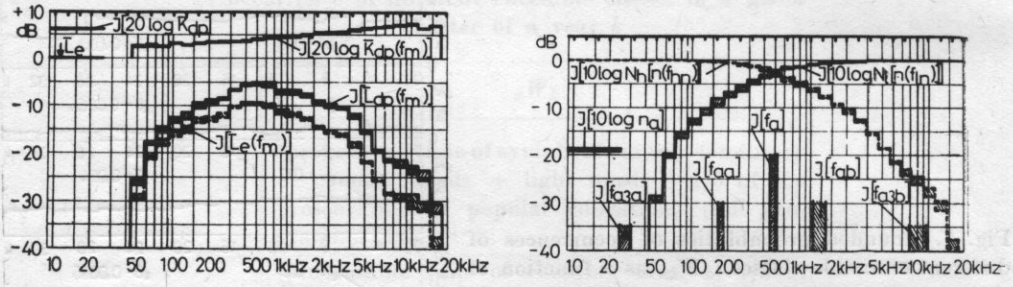

Fig. 8 a, b. Intervals of long-time-averaged statistical properties of programme signals weighted by ${}_xW$, the rounded mean probability of occurrence of different ensemble classes, averaged over the three different transmitted programmes. Values of the weights are given in Table III

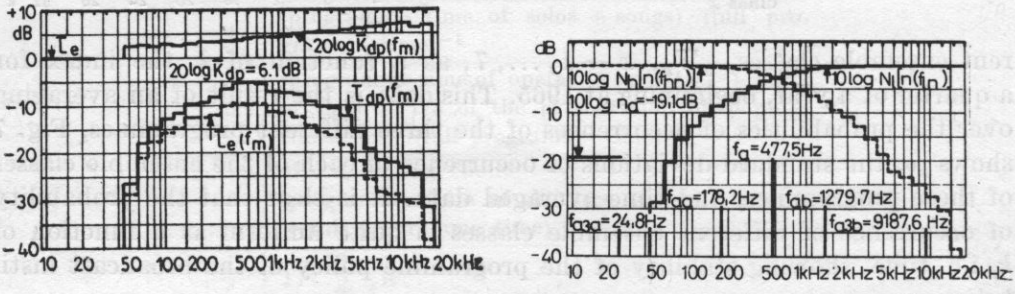

Fig. 9 a, b. Statistical properties of the long-time-averaged programme signal

Taking the data of Table 3 into consideration we can say generally that the bandwidth Δf of a programme signal is particularly dependent on the probability of music occurring rather than speech, i.e. of the ratio ${}_7W(1-{}_7W)^{-1}$. The smaller this ratio is, approximately, the wider will be the bandwidth Δf. There is also another interesting consequence: a diminution of this ratio causes a growth of the first spectral moment f_a.

Thus it is evidently possible to define a hypothetical programme in which the probability of the occurrence of different ensemble classes are the averages of the values obtained for these three different programmes. The mean values of these averages are given in the last column of Table 3. Using these average

Table 3. Rounded mean probabilities, ${}_xW$, and standard deviations ${}_x\sigma$, of the occurrence ${}_xW_k$, of different ensemble classes in different transmitted programmes

${}_xW$ / ${}_x\sigma$	Marks of transmitted programmes			
	No. 1	No. 2	No. 3	Averages
${}_1W$	0 20	0 26	0.31	0.26
${}_1\sigma$	0.043	0.039	0.035	0.022
${}_2W$	0.03	0.04	0.12	0.06
${}_2\sigma$	0.0064	0.0096	0.028	0.013
${}_3W$	0.23	0.21	0.15	0.19
${}_3\sigma$	0.052	0.047	0.035	0.032
${}_4W$	0.02	0.03	0.06	0.04
${}_4\sigma$	0.005	0.0044	0.016	0.0065
${}_5W$	0.10	0.11	0.18	0.13
${}_5\sigma$	0.014	0.015	0.03	0.054
${}_6W$	0.01	0.01	0.02	0.01
${}_6\sigma$	0.0025	0.003	0.011	0.0035
${}_7W$	0.41	0.34	0.16	0.31
${}_7\sigma$	0.036	0.041	0.054	0.037

values for weights, we have calculated the weighted long-time-averaged statistical properties in the same manner as discussed above. The results are shown in Figs. 9*a*, 9*b*. These are really averages in all respects because we have first averaged in a given ensemble group, using 24 independent samples of the programme signals, characteristic of the ensemble group considered; then we have averaged data between ensemble groups and thereafter we have weighted these averaged values with an averaged programme statistics where the last averaging procedure has been made using data from 34 quarter years and from three different transmitted programmes. Our procedure therefore justifies calling the data obtained the long-time programme signal.

We should mention that calculating the weighted average values, regarding the probability of occurrence of different ensemble classes as equal, we obtain results having only small (one or two dB) differences from the values

weighted by the different or by the average programme statistics. Thus in general most of the spectral properties of the long-time-averaged programme signal are quite insensitive to the probability of occurrence of our ensemble classes. This is clearly a consequence of our using a considerable number of ensemble classes.

Spectrally equivalent programme signal

It is now possible to construct a spectrally equivalent programme signal, by which we mean the output of a linear, passive or active network fed by random noise of gaussian probability distribution and of constant power spectral density in the frequency range of at least 31.5 Hz - 16,000 Hz, where the frequency response of the network corresponds within close limits to the power spectral density of the long-time-averaged programme signal.

We have therefore calculated $\bar{L}_e(f)$, the power spectral density level of the long-time programme signal integrated power density level $\bar{L}_e(f_m)$, shown in Fig. 9*a*, simply by subtracting $10 \log \Delta f_m$, where Δf_m is the power bandwidth of the 1/3 octave bandwidth filter of mid-band frequency f_m. In order to obtain a filter as simple as possible, we have chosen for the tolerance limits of the spectral density function, the upper and lower curves drawn by the thin lines of Fig. 10. The calculated power spectral density level $\bar{L}_e(f)$ lies

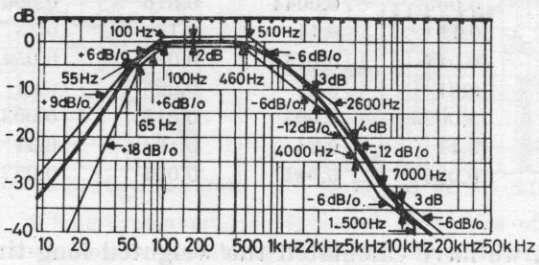

Fig. 10. Tolerance band of the spectrally equivalent programme signal. The curve drawn with a thick line is the power spectral density of a white noise signal weighted by the network of Fig. 11

approximately in the middle of this tolerance band. The curve drawn with a thick line on this figure shows the measured frequency response of the network shown in Fig. 11. Our tolerance band appears to be broad enough to have a simple network but also narrow enough to obtain practically a close approximation to the spectral density level of the long-time programme signal. The output of the network, fed by white noise, measured by using an 1/3 octave band-pass filter of Brüel & Kjaer Type 2112 is shown in Fig. 11. The results obtained for the 1/3 octave band levels in the bands from 63 Hz to 12.5 kHz

had midfrequency deviations of no more than 2 dB, referred to the levels $\bar{L}_e(f_m)$, shown in Fig. 9. Taking into consideration that the tolerance band of Fig. 10 contains all the results obtained for the three different programmes, as well as for the case of an equally weighted case, there seems to be no reason to make this tolerance band narrower.

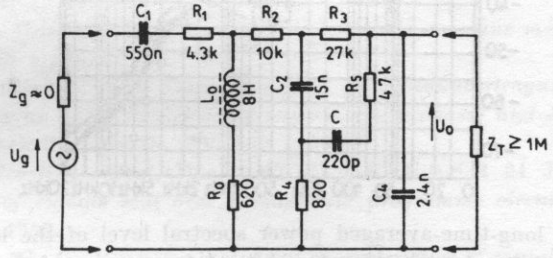

Fig. 11. A weighting network, fed by white noise, to obtain the spectrally equivalent programme signal. All component values are of tolerances of $\pm 1\%$. The power spectral density of the output signal of the network is shown by Fig. 10, thick line

Discussion

It is very interesting to compare our result expressed as a power spectral level to those existing in the literature. Fig. 12 shows (with a thick curve) our results and the thin lines are the proposed limits of the tolerance band. We have drawn data published in [13], Fig. 5, for two different programmes, measured and calculated taking into account the daily statistics of different kinds of programmes. Fig. 12 also shows the results of [14] Fig. 9. These have been obtained by measuring representative samples of normal broadcasting programme items (classical and light music, jazz and speech) having a duration proportional to their relative occurrence in the daily transmitted programme.

As Fig. 18 shows there is satisfactory agreement between the different results in the frequency range of 50 Hz-3 kHz but outside this range, the data shows quite large deviations (particularly that taken from [14], Fig. 9). This is very probably due to the small nummer of programme items as well as to the measurement and evaluation procedures used. The data given by [13], Fig. 5, shows, over the whole frequency range for which it has been published, i.e. from 40 Hz-8 kHz, good agreement with our data.

Unfortunately we have not found any other data published in the literature. Our results, and the data presented concerning the spectrally equivalent programme signal seem therefore to provide a solid base for future investigations.

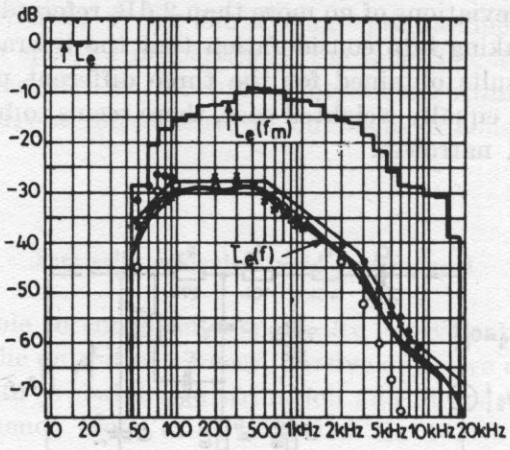

Fig. 12. $\bar{L}_e(f_m)$, the long-time-averaged power spectral level of the long-time programme signal, integrated in 1/3 octave bands of mid-band frequencies of $\bar{L}_e(f_m)$, the long-time-averaged power spectrum level of the long-time programme signal, both referred to $\bar{L}_e$, the long-time-averaged power of the unfiltered long-time programme signal. Points and circles are results of other investigations (see text)

× – data for transmitted programme No. 1, ● – data for another transmitted programme No. 2 Both are averaged for one day, After [12], Fig. 5, ○ – data of a transmitted programme signal, calculated for a year. After [14], Fig. 9. The thin curves border the tolerance band proposed for the spectrally equivalent programme signal

Acknowledgment. During this work, the writer has been encouraged by Mr. András Hartai, Technical Director of Elektroakusztikai Gyár, as well as by Mr Gábor Heckenast, Technical Director of Hungarian Radio. Thanks are also due to Mr. Tibor Szávai for writing the computer programme, to Miss Rozalia Szabó for drawing the figures, and to Mr Sándor Steinbach who mixed and edited the tapes used.

The editor wishes to express his gratitude to Prof. T. Tarnóczy for his assistance in preparing this paper for publication.

References

[1] I. B. Crandall, D. McKenzie, *Analysis of the energy distribution in speech*, Phys. Rev. Ser., **3**, 2, 221–232 (1922).

[2] L. J. Sivian, *Speech power and its measurements*, Bell Syst. Techn. Journ., **8**, 646–661 (1929).

[3] H. K. Dunn, S. D. White, *Statistical measurements on conversational speech*, JASA, **11**, 278–288 (1940).

[4] N. R, French, J. C. Steinberg, *Factors govering the intelligibility of speech sound*, JASA, **13**, 90–113 (1947).

[5] S. S. Stevens, J. P. Egan, G. A. Miller, *Methods of measuring speech spectra*, JASA, **19**, 771–780 (1947).

[6] Th. Tarnóczy, *Determination of the speech spectrum through measurements of superposed samples*, JASA, **28**, 1270–1275 (1956).

[7] W. Jassem, B. Piela, M. Steffen, *Average spectra of Polish speech*, Proc. Vibr. Probl., **1**, 59–70 (1959).

[8] G. Fant, *Acoustic analysis and synthesis of speech with application to Swedish*, Ericsson Techn., **15**, 3–108 (1959).

[9] L. J. Sivian, H. K. Dunn, S. D. White, *Absolute amplitudes and spectra of certain musical instruments and orchestras*, JASA, **2**, 330–371 (1931) (See also IRE Trans, on Audio **AU–7**, 47–75 (1959)).

[10] L. W. Young, H. K. Dunn, *On the interpretation of certain sound spectra of musical instruments*, JASA, **29**, 1070–1073 (1937).

[11] Th. Tarnóczy, *Determination du spectre de la parole avec une méthode nouvelle*, Acoustica, **8**, 392–395 (1958).

[12] G. Fischer, J. Rash, *Die bei Fernsprech- and Rundfunkübertragung auftretenden elektrischen Leistungen an unter Berücksichtigung von Preemphasis und Kompander*, Nachrichtentechn. Zeitschrift, Jg. 18, 205–209 (1965).

[13] *Power of broadcasting signal*, Doc. CMTT/153-*E*, U.S.S.R 21 July 1969.

[14] *Characteristics of signals sent over monophonic programme circuits*, Doc. CMTT/158-*E*, Italy 22 July 1969.

[15] L. W. Shitov, B. G. Belkin, *Statistical characteristics of signals of natural sounding and their use for measuring electroacoustical system* (in Russian), Trudy NIKFI, Bull. 56, 77–174 (1970).

[16] S. Ehara, M. Shibata, *Spectrum amplitude distribution of orchestra music* (in Japanese), N.H.K. Techn. Journ., **22**, 25–32 (1970).

[17] S. Ehara, *Spectrum amplitude distribution of orchestra music* (in Japanese), J. Acoust. Soc. Japan, **27**, 4, 214–224 (1971).

[18] *Unpublished memorandum of the author.*

[19] J. L. Doob, *Stochastic processes*, John Wiley and Sons, New-York 1962.

[20] J. E. Broch, *Effective averaging time of the level recorder type* 2305, Brüel & Kjaer Techn. Rev. 1, 3–23 (1961).

[21] *Programme statistics of the Hungarian radio*, Interim report, 1965, 1966, 1967, 1968, 1969, 1970, 1971, 1972, 1973.

Received on September 6, 1979.

ARCHIVES OF ACOUSTICS
5, 2, 143-146 (1980)

TIME ERROR IN PERCEPTION OF SOUND BRIGHTNESS

TOMASZ ŁĘTOWSKI, JACEK SMURZYŃSKI

Laboratory of Musical Acoustics, Chopin Academy of Music (00-368 Warszawa)

The paper presents the results of experiments in perception of sound brightness. The purpose of the investigation was to define paired comparison conditions in which the time error (TE) occurs. The duration of the interstimulus interval (ISI) between two white noise signals was used as an independent variable. No TE was observed for ISI of 0.1-2 s. A small negative TE occurred for longer ISI (4-8 s). Similar results were obtained for the noise stimuli limited in the low and high frequency range.

1. Introduction

One of the basic tasks of psychoacoustic experiments is to determine the thresholds of human auditory perception. As a threshold we understand the boundary separating stimuli producing one kind of human sensation from another. One of the standard methods used in threshold investigation is paired comparison procedure. When this method is applied the "time error" (TE) may be observed. The term *time error* refers to the systematic asymmetries that commonly arise in comparisons between stimuli which are presented pairwise, separated by a time interval. Numerous investigations have provided evidence that the TE is dependent upon several stimulus factors, particularly the length of the interstimulus interval (ISI), the level of stimulation etc. A sequential comparison of stimuli makes the evaluation dependent on both memory and masking factors. It can be generally assumed that the significance of the memory factor increases as the ISI increases and the significance of the masking factor is the greatest for short ISIs. The minimalization, or, at least, the knowledge of the character of the TE, is necessary to draw valid conclusions from the results obtained.

In the design of the test special control tasks in which both of the stimuli compared are objectively the same are used to disclose the TE character. TE is assumed as equal to zero when both stimuli in control tasks are judged as identical by the listeners. TE is assumed to have a negative or positive value if the investigated feature in the first stimulus is under- or overestimated, respectively, in relation to the second.

Some data on the auditory time errors for loudness and pitch perception can be found in psychological and acoustic literature. As for the loudness the first information on this subject was given by KÖHLER [3], who noticed a positive TE for ISI of 1.5 s, practically zero TE at 3 s and a negative TE at 6 and

12 s. POSTMAN [8] obtained fairly similar results founding a positive TE for ISI of 1 and 2 s but a negative TE with longer intervals (4 and 6 s). In 1954 POLLACK [7] carried out a very extensive study on the loudness perception confirming the general character of the TE as had been determined by the previous workers. However, the range of ISI values in which TE ≈ 0 was found as lying slightly lower than had been assumed before. Depending on the method used to compare stimuli and the experimental setting, the time varies from 0.65 s to 2.5 s (1.25 s on the average). A similar conclusion can be drawn from NEEDHAM's paper [6] (TE = 0 for ISI of 1-1.5 s).

When the pitch of tones is judged there is no agreement between investigators as to the existence of TE. TRUMAN and WEVER [9], KOESTER [4] and POSTMAN [8] carried out several series of investigations using various methods. Neither of these investigators was able to demonstrate any time error, positive or negative, for any of their subjects for ISIs shorter than 6 s. These results, however, are in disagreement with the observations of MASSARO [5], JAROSZEWSKI and RAKOWSKI [1], who have shown the existence of a positive TE for ISI shorter than 300 ms.

All the data mentioned above deal with the TE in the case of two physically identical stimuli being compared. When pairwise stimuli differ from one another in respect of an investigated feature, the listeners have an additional tendency to overestimate the existing difference both in the loudness and in the pitch perception tasks.

However, there are still no data on the TE occurring in a sequential comparison of sound timbre. This became especially important nowadays due to an increasingly wide interest in multidimensional scaling of timbre and the development of sound quality evaluation method. For that reason an experiment on the TE for timbre perception was carried out. In regard to preliminary assessment of this problem subjects were only questioned on one dimension of timbre, namely brightness of sound.

2. Procedure and results

Wide band noise was the signal in the experiment. Two seconds long samples of the signal were paired compared in respect to brightness of sound impression. In each sequence two stimuli were separated with ISI equal respectively to 0.1, 0.2, 0.5, 1, 2, 4 and 8 s. The test consisted of 84 trials. A white noise signal was a reference stimulus (designated "0"). For each value of ISI four "0–0" type test sequences were presented (28 trials). In the other trial sone of the stimuli was high-pass or low-pass noise with cut-off frequency respectively 14.1 kHz (signal "1") or 11.2 kHz (signal "2") and 141 Hz (signal "3") or 178 Hz (signal "4"). All high- and low-pass signals were produced from the reference stimulus with the help of Brüel-Kjaer Spectrum Shaper 5587. All sequencies 0–1, 1–0, 0–2, 2–0 etc. were presented once for each

of the investigated ISI values. All 84 trials in the test were presented at random. The pause between successive trials was equal to 5 s. Each trial was preceded by a short pulse of 1 kHz sine wave. The duration of the whole test was about 16 minutes.

The test was recorded on and played back from — Revox *A77* tape recorder. Test signals were reproduced with the help of two parallelly working "Fonia" GK-132 sound monitors. The frequency range of electroacoustic chain was equal to 40-18000 Hz±3 dB. The sound control room at the Chopin Academy of Music in Warsaw was used as a listening room.

The test was presented at loudness level of 80 phones. The subjects were 15 students and faculty members of the Sound Recording Department. All subjects had normal hearing acuity and some previous experience in psychoacoustic experiments. The age ranged from 20 to 35 years. The listeners' task was to determine which of the two stimuli in each trial was perceived as "brighter". The subjects could not answer: "I don't know" or "Both stimuli are identical".

The results obtained are presented in Tables 1 and 2. Based on Tables 1 and 2, a statistical analysis of the results was performed. Experimental results were compared against the hypothesis that the choice of the first or the second signal in a pair was equally probable. The test for significance of a proportion

Table 1. Experimental results for "0-0" type trials

ISI [s]	Proportion of the choice of the first or the second stimulus in a pair	The value of z statistics
0.1	27 : 33	−0.77
0.2	34 : 26	1.03
0.5	33 : 27	0.77
1.0	35 : 25	1.29
2.0	25 : 35	−1.29
4.0	20 : 40	−2.58
8.0	18 : 42	−3.10

Table 2. Experimental results for mixed pairs trials

ISI [s]	Proportion of the choice of the first or the second stimulus in a pair for trials							
	0–1	1–0	0–2	2–0	0–3	3–0	0–4	4–0
0.1	13 : 2	1 : 14	14 : 1	1 : 14	1 : 14	15 : 0	0 : 15	15 : 0
0.2	12 : 3	1 : 14	14 : 1	0 : 15	0 : 15	15 : 0	1 : 14	15 : 0
0.5	13 : 2	4 : 11	15 : 0	0 : 15	0 : 15	14 : 1	1 : 14	14 : 1
1.0	9 : 6	4 : 11	15 : 0	0 : 15	0 : 15	14 : 1	1 : 14	14 : 1
2.0	9 : 6	1 : 14	14 : 1	0 : 15	0 : 15	14 : 1	1 : 14	15 : 0
4.0	10 : 5	4 : 11	15 : 0	0 : 15	0 : 15	12 : 3	1 : 14	12 : 3
8.0	9 : 6	2 : 13	15 : 0	0 : 15	2 : 13	11 : 4	0 : 15	13 : 2

(z-test) was made at a significance level $\alpha = 0.1$ [2]. The results are presented in the third column of Table 1. The z-values obtained for ISI of 0.1-2 s satisfied the condition $|z_{emp}| < z_{0.05} = 1.645$ indicating the lack of the TE for the evaluation of sound brightness.

For ISI equal to 4 and 8 s, $|z_{emp}| > z_{0.05} = 1.645$ indicates the occurrence of the TE under the experimental conditions.

The results presented in Table 2 testify that all four low- and high-pass conditions had distinctly audible character. It was the most difficult in terms of sound brightness to distinguish "1" from "0" signals. Error distribution in 0—1 or 1—0 (30 : 17) and 0—3 or 3—0 (3 : 20) sequences indicates that listeners generally tended to evaluate the second stimulus in the pair as brighter. The differences in errors are significant at a level $\alpha = 0.1$ in both cases. This observation agrees with the results of the analysis for "0—0" type trials.

3. Discussion

The data shown in Tables 1 and 2 indicate the lack of the distinct TE for sound brightness for ISI of 0.1-2 s. The error distributions obtained for "0—0" conditions prove the random distribution of responses. Longer ISIs indicate the existence of negative value of the TE. One can state that the subjects overestimate brightness of sound for the second stimulus. It seems to justify the hypothesis that auditory memory is better for lower than for higher components of the spectrum. This hypothesis requires, however, to be confirmed by subsequent experimental investigations.

For mixed pairs of stimuli the subject perceived correctly all differences in brightness. The total number of errors did not exceed 10% (76 errors). Moreover, the distribution of errors shows that the difficulty of the test increases according to the value of ISI.

References

[1] A. Jaroszewski, A. Rakowski, *Pitch shifts in poststimulatory masking*, Acustica, 34, 220–223 (1976).

[2] J. P. Guilford, *Fundamental statistics in psychology and education*, McGraw-Hill Book Co. Inc., 1959.

[3] W. Köhler, *Zur Theorie des Sukzessivvergleichs und der Zeitfehler*, Psychol. Forsch. 4, 115–175 (1923).

[4] T. Köster, *Time-error and sensivity in pitch and loudness discrimination as a function of time interval and stimulus level*, Arch. Psychol. N. Y., 297 (1945).

[5] D. W. Massaro, *Perceptual processing time in audition*, JASA, 57, S 5 (A) (1975).

[6] J. G. Needham, *The time error as a function of continued experimentation*, Am. J. Psychol., 46, 558–567 (1934).

[7] I. Pollack, *Intensity discrimination thresholds under several psycho-physical procedures*, JASA, 26, 1056–1059 (1954).

[8] L. Postman, *The time-error in auditory perception*, Am. J. Psychol., 59, 193–219 (1946).

[9] S. R. Truman, E. G. Wever, *The judgment of pitch as a function of series*, Calif. Univ. Publ. Psychol., 3, 215–223 (1928).

Received on May 16, 1979.

ARCHIVES OF ACOUSTICS
5, 2, 147-156 (1980)

INFLUENCE OF RIBS ON THE ACOUSTIC BEHAVIOUR OF PIANO RESONANT PLATES

U. MÜLLER

Institut für Musikinstrumentenbau (9657, Zwota GDR)

The eigenfrequencies and vibrational modes of a simply supported stiffened rectangular plate are determined by means of perturbation method. Additional eigenmodes are excited by the presence of ribs and the eigenfrequencies are shifted. A qualitative evaluation of the influence of these additionally excited modes on the sound radiated shows that under certain conditions the ribs can improve the sound radiation of a resonant plate.

Glossary of symbols

E — modulus of elasticity
h — plate thickness
σ — Poisson's ratio
Δ^2 — biharmonic operator
ξ — vibrational displacement of plate
ϱ — density of plate material
t — time
ω — angular frequency
$\vec{n}$ — unit vector in a normal direction
x, y — Cartesian coordinates
a, b — plate dimensions in the x- and y- directions respectively
ψ_{mn} — eigenfunctions of the biharmonic operator
ω_{mn} — eigenfrequencies of the non-stiffened plate
i, k, m, n, r, s — integers
ξ_{ik} — eigenfunctions of the stiffened plate
V, L — perturbation quantities
$Sch(x,y)$ — switch function
d — thickness of the ribs
J — second order moment of the rib area
S_R — cross-sectional area of the ribs
a_{mnik} — coefficient
$\omega_{ik}^{(N)}$ — N-th approximation of the eigenfrequency of the stiffened plate vibrating in the (i, k) mode

$\omega_R(k)$ – eigenfrequency of the ribs vibrating in the (k) mode
h_R – rib height
k_S – wave number of the acoustic field
j – $j^2 = -1$
p – sound pressure
u'_{ik} – velocity of the stiffened plate vibration, (i, k) mode
u_{mn} – velocity of the unstiffened plate vibration, (m, n) mode
p'_{ik} – sound pressure generated by the stiffened plate, vibrating in the (i, k) mode
p_{mn} – sound pressure generated by the unstiffened plate, vibrating in the (m, n) mode
r, ϑ, φ – polar coordinates
ϱ_L – density of air
c – sound velocity
k_B – plate bending wave number
P – acoustic power radiated
S – radiation efficiency

1. Introduction

A large number of methods for calculating the vibrational modes and eigenfrequencies of stiffened plates have been published previously. Two papers which are of special interest for the present purpose will be mentioned here: KIRK [1] determined the natural frequencies of the first symmetric and the first antisymmetric modes of a simply supported rectangular plate which is reinforced by a single integral stiffener placed along one of its centre lines; while KOVINSKAJA and NIKOFOROV [2] investigated the field of flexural waves on an infinite point excited plate with two or three ribs.

There are also a large number of papers dealing with the interaction of flexural waves on a stiffened plate with the acoustic field in the surrounding room. MAIDANIK [3] used a statistical method for estimating the response of ribbed panels to acoustic excitation. ROMANOV [4] and [5] calculated the sound radiation from an infinite stiffened plate which is excited by a stochastic force between the ribs, and EVSEEV [6] discussed the sound radiation from an infinite plate excited by a harmonic force. All these papers show the immense mathematical difficulties which are connected with the theoretical treatment of the vibrations of a stiffened plate, and the sound field generated by these vibrations.

For this reason, simplifications have to be made, and these are determined by the intended practical application of the results. In order to investigate the acoustic behaviour of resonant plates in musical instruments, the eigenmodes and eigenfrequencies of a rectangular simply supported stiffened plate will be determined. The ribs are assumed to be parallel to one boundary of the plate. Both assumptions: the simple boundary conditions and a simple arrangement of the ribs, are necessary to make the problem mathematically manageable, without lengthy digital computation.

2. Eigenmodes and eigenfrequencies of a stiffened plate

Flexural waves on a thin plate may be described by the differential equation

$$\frac{Eh^3}{12(1-\sigma^2)}\Delta^2\xi+\varrho h\frac{\partial^2\xi}{\partial t^2}=0.$$

This equation is derived for instance in [7] and [8]. We confine the discussion to sinusoidal time dependence. Thus differentiation with respect to time may be replaced by $+j\omega$. This leads to

$$\frac{Eh^3}{12(1-\sigma^2)}\Delta^2\xi-\omega^2\varrho h\xi=0.$$

In order to determine the eigenmodes of a finite plate this differential equation has to be solved with consideration of the boundary conditions. In the case of a simply supported plate, the displacement and bending moment are zero at the boundaries:

$$\xi=0 \quad \text{and} \quad \frac{\partial^2\xi}{\partial\vec{n}^2}=0.$$

For a rectangular plate with boundaries at $x=0$ and $x=a$ and $y=0$ and $y=b$ we can write these equations as

$$\frac{Eh^3}{12(1-\sigma^2)}\left[\frac{\partial^4}{\partial x^4}+2\frac{\partial^4}{\partial x^2\partial y^2}+\frac{\partial^4}{\partial y^4}\right]\xi-\omega^2\varrho h\xi=0,$$

$\xi=0$ if $x=0$, or $x=a$, or $y=0$, or $y=b$; $\partial^2\xi/\partial x^2=0$ if $y=0$, or $y=b$; $\partial^2\xi/\partial y^2=0$ if $x=0$, or $y=a$.

The solution of this eigenvalue equation is

$$\psi_{mn}=\frac{2}{\sqrt{ab}}\sin\frac{m\pi}{b}x\sin\frac{n\pi}{b}y$$

$$(0\leqslant x\leqslant a;\ 0\leqslant y\leqslant b;\ m,n=1,2,3,\ldots) \tag{2}$$

with eigenvalues

$$\omega_{mn}=\sqrt{\frac{Eh^2}{12\varrho(1-\sigma^2)}\left[\left(\frac{m\pi}{a}\right)^2+\left(\frac{n\pi}{b}\right)^2\right]}. \tag{3}$$

The ribs influence the plate vibrations by virtue of their stiffness and inertial mass. Since, however, these are assumed to be small compared with the stiffness and inertia of the plate itself, the use of a perturbation method is justified. The differential equation for a stiffened plate may then be written as

$$\left[\frac{Eh^3}{12(1-\sigma^2)}\Delta^2+V-(1+L)\varrho h\omega_{ik}\right]\xi_{ik}=0. \tag{4}$$

$V\xi_{ik}$ is the stiffness force and $L\varrho h\omega_{ik}\xi_{ik}$ – the inertial mass force of the ribs which act on the plate. For ribs parallel to the y-axis we have

$$V = \frac{EJ}{d}\,\mathrm{Sch}(x)\,\frac{\partial^4}{\partial y^4} \quad \text{and} \quad L = \frac{S_R}{\varrho h}\,\mathrm{Sch}(x).$$

$\mathrm{Sch}(x)$ is a switch function with a values of 1 at the places where there are ribs and 0 elsewhere.

The eigenfunctions ψ_{mn} of the plate differential equation (1) form a system of normalized orthogonal functions. It is therefore possible to find the solution of equation (4) in terms of a series:

$$\xi_{ik} = \sum_{m,n} \psi_{mn} a_{mnik}. \tag{5}$$

According to the assumptions of perturbation method all the terms except that with ψ_{ik} are small. This is identical with the statement that a stiffened plate vibrates essentially like the corresponding unstiffened plate, but with some small amplitude vibration of additionally excited eigenmodes, i.e. for every approximation N, $a_{ikik}^{(N)} = 1$. The other coefficients a_{mnik} are calculated by means of an iteration method which is performed by inserting the series (5) into the differential equation (4) of the stiffened plate:

$$\omega_{ik}^{(N)} = \frac{\omega_{ik}^{(0)2} + \sum\limits_{rs} V_{ikrs}\, a_{rsik}^{(N-1)}}{1 + \sum\limits_{rs} L_{ikrs}\, a_{rsik}^{(N-1)}}, \tag{6}$$

$$a_{mnik}^{(N)} = \frac{\sum\limits_{rs} V_{mnrs}\, a_{rsik}^{(N-1)} - \omega_{ik}^{(N)2} \sum\limits_{rs} L_{mnrs}\, a_{rsik}^{(N-1)(N-1)}}{\omega_{mn}^{(0)2} - \omega_{ik}^{(N)2}}, \tag{7}$$

with

$$V_{mnrs} = \int_0^a \int_0^b \psi_{mn} V \psi_{rs}\, dx\, dy, \qquad L_{mnrs} = \int_0^a \int_0^b \psi_{mn} L \psi_{rs}\, dx\, dy.$$

The method is started in the zeroth approximation with

$$\omega_{ik}^{(0)} = \omega_{ik},$$

$$a_{mnik}^{(0)} = \begin{cases} 1 & \text{for } m = i \text{ and } n = k, \\ 0 & \text{otherwise.} \end{cases}$$

We note that in the zeroth approximation, the eigenfrequencies and vibrational modes of a stiffened and an unstiffened plate are the same. Insertion of the zeroth approximation into equation (6) yields the eigenfrequencies of the stiffened plate in the first approximation, and this inserted in turn into equation (7) yields the coefficients a_{mnik} in the first approximation. Using the first approximation and equations (6) and (7) we may obtain the second one

and so on. If some of the eigenmodes of the differential equation (1) of the plate are degenerate, i.e. they have the same eigenfrequency, some of the coefficients a_{mnik} become infinite, and the series (5) diverges. The problem may be made manageable by using linear combinations of the degenerate modes in such a manner that the corresponding V_{mnik} and L_{mnik} become zero and the diverging terms are eliminated.

Let us assume that the ribs are situated at x_ν and their thickness is small compared with the flexural wave length, so that we have

$$V_{mnrs} = \frac{2EJ}{\varrho a h}\left(\frac{s\pi}{b}\right)^4 \sum_\nu \sin\frac{m\pi}{a}x_\nu \sin\frac{r\pi}{a}x_\nu \delta_{ns},$$

$$L_{mnrs} = \frac{2S_R}{ah}\sum_\nu \sin\frac{m\pi}{a}x_\nu \sin\frac{v\pi}{a}x_\nu \delta_{ns},$$

where

$$\delta_{ns} = \begin{cases} 1 & \text{for } n = s \\ 0 & \text{otherwise.} \end{cases}$$

The first approximation is then written as

$$\omega_{ik}^{(1)^2} = \frac{\omega_{ik}^{(0)^2} + \dfrac{2EJ}{ah}\left(\dfrac{k\pi}{b}\right)^4 \sum_\nu \left(\sin\dfrac{i\pi}{a}x_\nu\right)^2}{1 + \dfrac{2S_R}{ah}\sum_\nu \left(\sin\dfrac{i\pi}{a}x_\nu\right)^2},$$

$$a_{mnik}^{(1)} = \frac{\dfrac{2S_R}{ah}\left[\dfrac{EJ}{\varrho S_R}\left(\dfrac{k\pi}{b}\right)^4 - \omega_{ik}^{(1)^2}\right]\sum_\nu \sin\dfrac{m\pi}{a}x_\nu \sin\dfrac{i\pi}{a}x_\nu \delta_{ns}}{\omega_{mn}^2 - \omega_{ik}^{(1)^2}}.$$

Using the eigenfrequency equation of the ribs,

$$\omega_R^2(k) = \frac{EJ}{\varrho S_R}\left(\frac{k\pi}{b}\right)^4,$$

the first approximation is written as

$$\omega_{ik}^{(1)^2} - \omega_{ik}^{(0)^2} = \frac{2\dfrac{S_R}{ah}\sum_\nu \left(\sin\dfrac{i\pi}{a}x_\nu\right)^2}{1 + \dfrac{S_R}{ah}\sum_\nu \left(\sin\dfrac{i\pi}{a}x_\nu\right)^2}\left(\omega_R^2(k) - \omega_{ik}^{(0)^2}\right),$$

$$a_{mnik}^{(1)} = \frac{2\dfrac{S_R}{dh}\sum_\nu \sin\dfrac{m\pi}{d}x_\nu \sin\dfrac{i\pi}{a}x_\nu}{\omega_{mn}^{(0)^2} - \omega_{ik}^{(1)^2}}\left(\omega_R^2(k) - \omega_{ik}^{(0)^2}\right).$$

From the equations it can be seen that eigenfrequencies are shifted by the ribs and additional eigenmodes are excited. The vibration amplitude of these additionally excited modes is much smaller than that of the original mode (in which the plate would vibrate if it had no ribs).

If the eigenfrequencies of the ribs for a given y-component $k\pi/b$ of the flexural wave number are smaller than the corresponding eigenfrequencies ω_{ik} of the unribbed plate, the eigenfrequencies $\omega_{ik}^{(N)}$ of the ribbed plates are smaller than those of the unribbed one, and the interaction of ribs and plate is mass controlled. For higher rib eigenfrequencies, the eigenfrequencies of the ribbed plate are higher than those of the unribbed one, and the interaction is stiffness controlled. If an eigenfrequency of the plate is equal to the corresponding eigen-

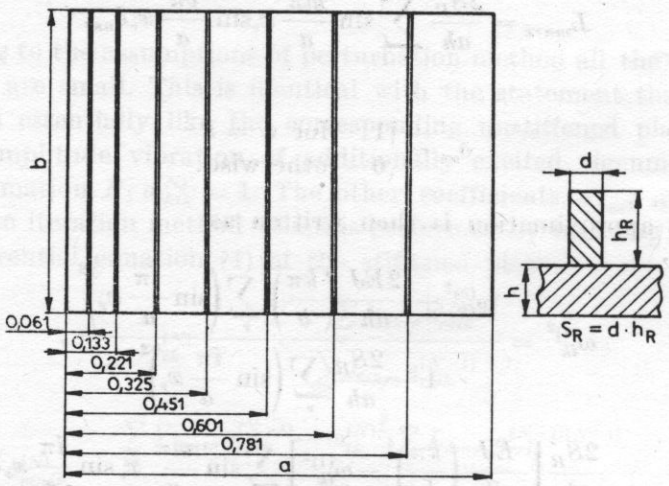

Fig. 1. The distribution of ribs on the plate

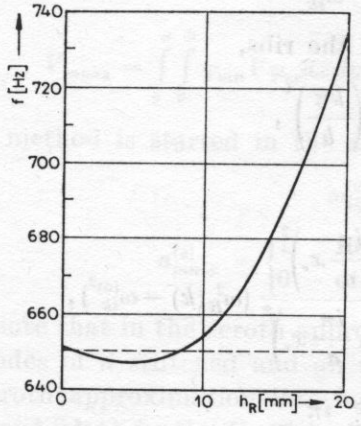

Fig. 2. Eigenfrequency of mode (6,6)

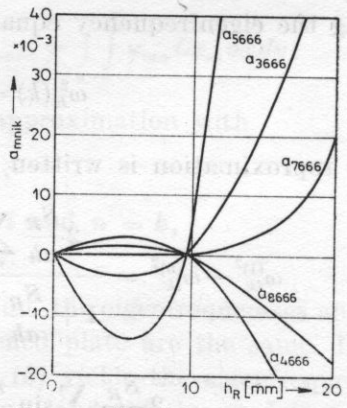

Fig. 3. Coefficients a_{mnik} for mode $(i, k) = 6,6$ (for $n \neq 6$, $a_{mnik} = 0$)

frequency of the ribs, the frequency shift (and the amplitudes of the additionally excited modes) become zero.

The calculation of the coefficients a_{mnik} shows that if the ribs are equidistant only a few modes are additionally excited, and most of the a_{mnik} become zero. In the case of nonequidistant ribs a large number of modes is excited.

The eigenfrequency $\omega_{ik}^{(1)}$ and the coefficients $a_{mnik}^{(1)}$ of the plate shown in Fig. 1 are given in Figs. 2 and 3 for the (6,6) mode for different rib heights. It can be seen that for $h_R < 9$ mm the ribs act like an additional mass. The eigenfrequency is lower than that of the corresponding unribbed plate, the coefficients $a_{m6\,66}$ are positive for even m and negative for odd m. For $h_R > 9$ mm the ribs act like an additional stiffness. The eigenfrequency is larger than that of the corresponding unribbed plate, and the coefficients $a_{m6\,66}$ are positive for odd m and negative for even m.

3. Sound radiation

The acoustic wave radiated by a baffled panel can be found from Rayleigh's integral. The acoustic pressure in the farfield produced by a harmonically vibrating plate can be obtained from the integral

$$P'_{ik}(r,\vartheta,\varphi) = -jks\varrho_L c\,\frac{e^{jksr}}{2\pi r}\int_0^b\int_0^a u'_{ik}(x,y)\exp\left[-j\left(\frac{dx}{a}\right)-j\left(\frac{\beta y}{b}\right)\right]dx\,dy, \tag{8}$$

where

$$\alpha = k_S a\sin\vartheta\cos\varphi,$$
$$\beta = k_S b\sin\vartheta\sin\varphi,$$

r, ϑ and φ are the polar coordinates of the field point and u'_{ik} is the surface velocity distribution which, in our case, may be written in terms of the series

$$u'_{ik} = j\omega\sum_{m,n}\psi_{mn}a_{mnik} = \sum u_{mn}a_{mnik}.$$

The sum represents the vibrational modes of the plate from which the velocity distribution is obtained by differentiation with respect to time (in case of harmonic vibration this means multiplication by $j\omega$). Thus the sound pressure may be expressed in terms of a series

$$p'_{ik} = \sum_{m,n} p_{mn}a_{mnik},$$

where p_{mn} is the sound pressure generated by the velocity distribution u_{mn}, which is the velocity distribution of a harmonically vibrating unstiffened plate in the (m, n) mode. The sound pressure field of a stiffened plate vibrating harmonically in the (i, k) mode is the superposition of the sound pressure fields of the corresponding unstiffened plate vibrating in several modes (m, n) with amplitudes a_{mnik} at the same frequency ω.

The radiated power may be calculated from the formula

$$P_{ik} = \int_0^{2\pi} \int_0^{\pi/2} \frac{|p_{ik}|^2}{\varrho_L c} r^2 \sin\vartheta d\vartheta d\varphi,$$

which leads, for the stiffened plate, to

$$P_{ik} = \int_0^{2\pi} \int_0^{\pi/2} \frac{|p_{ik}|^2}{\varrho_L c} r^2 \sin\vartheta d\vartheta d\varphi + \int_0^{2\pi} \int_0^{\pi/2} \frac{\sum_{r,s\neq(m,n)} p_{mn} p^*_{r,s} a_{mnik} a_{rsik}}{\varrho_L c} r^2 \sin\vartheta d\vartheta d\varphi + \int_0^{2\pi} \int_0^{\pi/2} \frac{\sum_{m,n\neq(i,k)} |p_{m,n}|^2 a^2_{mnik}}{\varrho_L c} r^2 \sin\vartheta d\vartheta d\varphi, \tag{9}$$

where p^*_{rs} is the complex conjugate of p_{rs}. The first term represents the power which would be radiated by the corresponding unstiffened plate vibrating in the (i, k) mode, and the third term represents the power radiated by the additionally excited modes. The second term results from the interaction of the different modes.

The influence of the ribs on the sound radiated by a stiffened plate may be understood by investigating the second and third terms of [9]. For this purpose the results obtained by WALLACE [9], who analyzed the radiation resistance of a rectangular panel, are very useful. Wallace studied the energy radiated by a mode of a harmonically vibrating simply supported panel, in the farfield.

For high frequencies, if $k_S/k_B \gg 1$, the radiation efficiency S is equals to one. For low frequencies, if $k_S/k_B \ll 1$, when m and n are both odd integers, the radiation efficiency is proportional to the square of the ratio of the corresponding wave numbers, $S \sim (k_S/k_B)^2$, when m is odd and n is even or, vice versa, $S \sim (k_S/k_B)^4$, and, when m and n are both even integers, $S \sim (k_S/k_B)^6$.

Since $a_{mnik} \ll 1$ for $n \neq i$ and $n \neq k$ the ribs can have a substantial influence only when the mode in which the unstiffened plate would vibrate radiates comparatively little energy and the additionally excited modes have a relatively high radiation efficiency. For example, for modes with both indices even, the first term of equation (9) is small, and the second has a dominating influence, for $k_S/k_B \ll 1$, if modes with one or both indices odd are excited. If, for odd m,

$$a_{mnik} a_{ikik} = a_{mnik} > 0,$$

that is if the plate ribs interaction is stiffness controlled ($h_R > 9$ mm in our example), the ribs enhance the radiation of sound in modes which originally had a small radiation efficiency.

If, for odd m,

$$a_{mnik}a_{ikik} = a_{mnik} < 0,$$

i.e. if the plate ribs interaction is mass controlled ($h_R < 9$ mm in our example), the ribs diminish the radiation of sound in modes with a small radiation efficiency.

4. Conclusions

Ribs cause an eigenfrequency shift. Ribs of small height diminish the plate eigenfrequencies, while ribs of large height increase the eigenfrequencies. In the first case the plate ribs interaction is mass controlled, and in the second one stiffness controlled. In addition, the ribs modify the sound radiation of the plate, in particular for those modes which originally have a low radiation efficiency (modes with both indices even and to some extent modes with one index even and one index odd in the low-frequency region, $k_S/k_B \ll 1$). Ribs of small height diminish sound radiation, ribs of large height enlarge the sound radiation in these modes. However, this effect is significant only in the case of nonequidistant ribs. Thus it is possible, in principle, to equalize the frequency response of the plate by adjusting the heights and spacings of the ribs.

References

[1] C. L. Kirk, *Natural frequencies of stiffened rectangular plates*, J. Sound Vib., **13**, 4, 375–388 (1970).

[2] S. J. Kovinskaja, A. S. Nikiforov, *Pola izgubnych voln v beskonečnych plastinach, podkreplennych rebrami žëstkosti pri točečnom vozbuždenii konstrukcii*, Ak. Žur., **XIX**, 1, 47–52 (1973).

[3] G. Maidanik, *Response of ribbed panels to reverberant acoustic fields*, JASA, **34**, 6, 809–826 (1962).

[4] V. N. Romanov, *Izlučenie zvuka beskonečnoj plastinoj pri naličii na nej reber žestkosti*, Ak. Žur., **XVII**, 1, 116–121 (1971).

[5] V. N. Romanov, *K voprosu ob izlučenii zvuka beskonečnok plastinoj s rebrami žëstkosti*, Ak. Žur., **XVIII**, 4, 602–607 (1972).

[6] V. N. Evseev, *Izlučënie zvuka beskonecnoj plastinoj s periodičeskimi neodnorodnostjami*, Ak. Žur., **XIX**, 3, 345–351 (1973).

[7] L. D. Landau, E. M. Lifschitz, *Lehrbuch der theoretischen Physik*, Bd. 7, Elastizitätstheorie, Berlin 1970.

[8] V. S. Gontkevič, *Sobstvennye kolebanija plastinok i oboloček*, Kiev 1968.

[9] C. E. Wallace, *Radiation resistance of a rectangular panel*, JASA, **51**, 312, 946–952 (1972).

Received on January 12, 1978; revised version on July 25, 1979.

ARCHIVES OF ACOUSTICS
5, 2, 157-168 (1980)

VERIFICATION OF THE METHOD FOR PREDICTION OF THE EQUIVALENT LEVEL OF FREELY FLOWING TRAFFIC NOISE

R. MAKAREWICZ, J. JARZĘCKI

Institute of Acoustics UAM (60-769 Poznań, ul. Matejki 48/49)

The evaluation of the "acoustic climate" near transport routes, using the numerical method is possible only when we know the values of the parameters describing single noise sources and those of the parameters connected with the attenuating properties of the area adjacent to the route. The paper presents a method for determining these parameters. Direct measurements of the equivalent level were also made. Good agreement between measurement results with values calculated according to the present analytical and theoretical method shows its correctness and thus its usefulness for the problem of shaping the acoustic environment near roads with freely flowing traffic.

1. Introduction

Noise is the cause of degradation of the environment. The measure of the degradation are the values of the noise indexes. One of these that is most often used, is the equivalent level — L_{eq}. The results from investigations, including those of LANGDON [12], SADOWSKI and SZUDROWICZ [23], show that means of transport are the most essential cause of noise pollution. They are the most annoying noise sources. The value of the equivalent level, L_{eq}, near transport routes depends, among other things, on:

— the parameters characterizing single vehicles as sources of acoustic field,

— numbers and velocities of vehicles passing the observation point in a time unit,

— the parameters determining the location of the transport route (e.g. distance from the observation point),

— the parameters characterizing the attenuating properties of the ground and of the air.

On the basis of the results from measurements of L_{eq} taken at different distances from a transport route, for various intensities and velocities of the traffic, using the regression method (see e.g. [4] or [6]), the relation

$L_{eq} = f(m_i)$, where m_i is a set of the above-mentioned parameters determining the value of the equivalent level L_{eq}, is obtained. It is rather labourious, since it requires a great many measurements of the value of L_{eq} for time intervals of several minutes duration.

The investigations performed aimed at developing a new method for determination of the relation $L_{eq} = f(m_i)$ (sections 2 and 3) and, subsequently, at its experimental verification (section 4).

Knowledge of the function $f(m_i)$ permits the quantity L_{eq} to be determined for different values of m_i, i.e. to evaluate the "acoustic climate" near a road with known traffic intensities and velocities of light and heavy vehicles, etc. (A full set of parameters m_i will be given later in the paper). This problem is particularly important for planners working on the transport network, i.e. when direct measurements of the equivalent level, L_{eq}, and a correct location of objects requiring particular noise protection, are impossible.

2. Theory

If the source is omnidirectional, then in open space filled with the ideal medium, the intensity I of the wave is a function of a distance r of the form

$$I = \frac{P}{4\pi r^2},$$

where P is the source power.

If the source moves near the plane, a direct wave and a reflected wave reach the observation point. In paper [16] an expression defining the intensity of the resultant wave was derived. It is a monotonically decreasing function of the distance r. The form of the function is very complicated, therefore it is convenient (similarly to FILOTAS [5] and LJUNGGREN [13], for example) to assume that

$$I = \frac{W}{4\pi r^{\varrho}}, \tag{1}$$

where W and ϱ are quantities depending on the acoustic parameters of the source and the reflecting plane, the attenuating properties of the medium (air) and the area separating the source from the observation point (e.g. tall trees or shrubs). Let us now consider the problem of the intensity of the field generated by a system of moving sources.

If the incoherent sources move on the plane (x, y) along linear paths, which are parallel to each other (Fig. 1), then the mean intensity of the resultant field [14, 15] at the observation point O is

$$\langle I \rangle = \frac{\sqrt{\pi}}{4\pi} \sum_{jk} \frac{\Gamma(\frac{1}{2}\varrho_{jk} - \frac{1}{2})}{\Gamma(\frac{1}{2}\varrho_{jk})} n_{jk} \frac{W_{jk}}{V_{jk}} \frac{1}{r_k \varrho_{jk} - 1} + I^{(0)}, \tag{2}$$

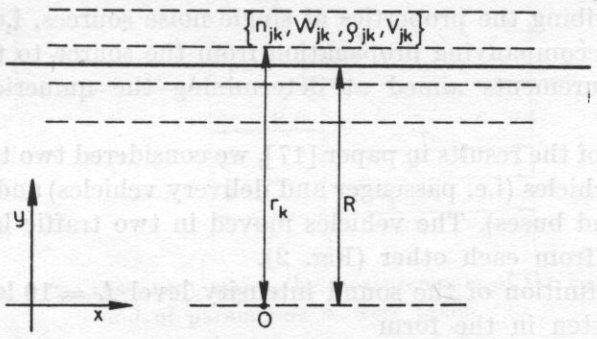

Fig. 1. Location of the observation point O with respect to the road (r_k – distance from traffic lanes, R – distance from the middle of the road)

where n_{jk} is the mean intensity of the traffic of the sources of the jth type along the kth path, V_{jk} is the mean velocity of the traffic of the sources of the jth type along the kth path, W_{jk}, ϱ_{jk} – the parameters related to the source of the jth type moving along the kth path, $\Gamma(x)$ is the Gamma function r_k is the distance of the observation point O from the kth path, $I^{(0)}$ is the mean intensity of the background.

The problem of the determination of the mean intensity $\langle I \rangle$ of the field generated by a system of moving sources was also investigated by ANDERSON [1], BLUMENFELD and WEISS [3], GORDON [7], JOHNSON and SAUNDERS [8], KUNO and IKEGAYA [9], KURZE [10], KUTTRUFF [11], LJUNGGREN [13], MARCUS [18], OHTA et al. [19], RATHE [22], SCHREIBER [24], TAKOGI et al. [25], ULLRICH [26], YEOW et al. [27], WEISS [28].

Relation (2) can be used for determining the equivalent level near roads with freely flowing traffic. According to PEARSON and BENNETT [20] we have

$$L_{\mathrm{eq}} = 10 \log \frac{\langle I \rangle}{I_0}, \tag{3}$$

where I_0 is the reference intensity, and

$$\langle I \rangle = \frac{1}{T} \int_0^T I(t)\,dt,$$

with T being the averaging time of arbitrary duration related to day, night or the whole 24 hours.

3. Experimental investigations of noise from single sources

To determine the value of L_{eq} according to formulae (2) and (3) it is necessary to know distances of the observation point from the paths, i.e. the lanes of traffic, r_k, the parameters of the traffic, n_{jk}, V_{jk}, and also the quantities

W_{jk} and ϱ_{jk} describing the properties of single noise sources, i.e. vehicles, and the phenomena accompanying propagation from the source to the observation point. Our measurements aimed at determining the numerical values W_{jk} and ϱ_{jk}.

On the basis of the results in paper [17], we considered two types of vehicles ($j=1, 2$): light vehicles (i.e. passenger and delivery vehicles) and heavy vehicles (trucks, lorries and buses). The vehicles moved in two traffic lanes ($k = 1, 2$), distant by 14 m from each other (Fig. 2).

Using the definition of the sound intensity level $L = 10 \log I/I_0$, relation (1) can be rewritten in the form

$$L_{jk} = a_{jk} - 10\varrho_{jk} x_k, \tag{4}$$

where

$$x_k = \log r_k, \quad a_{jk} = 10 \log \frac{W_{jk}}{4\pi I_0} \tag{5}$$

are the parameters related to the vehicle of the jth type, which moves along the kth path, with L_{jk} dB(A) being the acoustic pressure level (in this case the intensity level equals the pressure level [2]). In order to find the values of W_{jk} and ϱ_{jk} on the basis of relation (4), the measurements of L_{jk} were taken at distances $r_k (k = 1, 2$; Fig. 2) from the two traffic lanes, for light and heavy vehicles ($j = 1, 2$).

The values of L_{jk} were read when single vehicles "passed" the measurement point. The measurements were taken when the traffic intensity was low, so that the values of L_{jk} were the levels of intensity of signal actually emitted from the single vehicles.

The measurements of the levels L_{jk} corresponding to single light and heavy vehicles which moved on the nearest lane, L_{11} and L_{12}, were taken at distances $r_1 = 10, 20, \ldots, 60$ m. The readings were $N_{11} = 65$ and $N_{12} = 35$, respectively.

The measurements of levels L_{jk}, for light and heavy vehicles moving on the second lane, L_{21} and L_{22}, were taken at distances $r_2 = 24, 34, \ldots, 74$ m, with the numbers of vehicles being $N_{21} = 58$ and $N_{22} = 22$, respectively.

Having four sets at disposal $\{L_{jk}, r_k\}$ for $\{jk\} = \{11, 21, 12, 22\}$ and using the least squares analysis, the following numerical values a_{jk} and ϱ_{jk} (Table 1) were obtained from relation (4).

Table 1 also shows the mean traffic velocities V_{jk} and the correlation coefficients r. Then, using the same method for two sets $\{L_j, R\}$ with $\{j\} = \{1, 2\}$, the values of a_j and ϱ_j for light and heavy vehicles moving along the first or the second lane were determined (where the numbers of vehicles passing were respectively $N_1 = N_{11} + N_{12} = 123$, $N_2 = N_{21} + N_{22} = 57$, and $R = 17, 27, \ldots$ $\ldots, 67$ m (Fig. 2) were distances of the observation point O from the middle of the road). The results of the calculations of a_j and ϱ_j, the correlation coeffi-

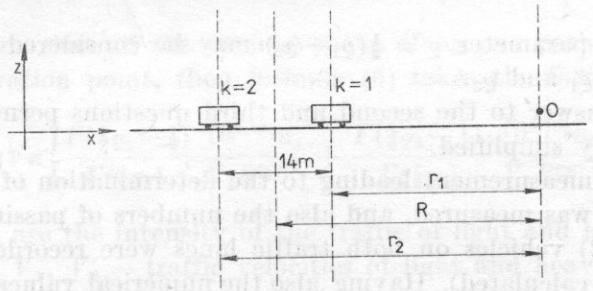

Fig. 2. Cross-section of the road near which the measurements of the equivalent level $L_{eq}^{(z}$ and of parameters a, were taken

cients and traffic velocities V_j for individual types of vehicles are shown in Table 2.

On the basis of the relations given above, and using Tables 1 and 2 the value of the equivalent level can be determined.

4. Measurements of the equivalent level of freely flowing traffic noise

When $\bar{L}_{eq}$ is the equivalent level of the background, from relations (2), (3), and (5) we obtain an expression which permits to determine the value of the equivalent level, L_{eq}, near a road with m lanes, on which vehicles move with a constant velocity:

$$L_{eq} = 10 \log \left\{ \sum_{j=1}^{2} \sum_{k=1}^{m} \pi \frac{\Gamma(\frac{1}{2}\varrho_{jk} - \frac{1}{2})}{\Gamma(\frac{1}{2}\varrho_{ik})} \frac{10^{0.1 a_{jk}}}{V_{jk}} \frac{n_{jk}}{r_k \varrho_{jk}} + 10^{0.1 L_{eq}} \right\}. \tag{6}$$

All the quantities on the right-hand side of the equation are measurable (the method for the measurement of parameters a_{jk} and ϱ_{jk} was discussed in section 3).

Taking into consideration the fact that a more precise division of vehicles (into types) than the one we spoke about before (light and heavy vehicles) is unnecessary [17], we assume that $j = 1, 2$. In the case considered here the road had two traffic lanes, i.e. $m = 2$.

The aim of direct measurements of L_{eq} near the same road (section 3) (for time intervals of five minutes for different distances r_k) was to answer the following three questions:

whether the method of prediction of L_{eq}, based on relation (6) is correct, i.e. whether the error committed in the calculation of L_{eq} is not too great,

whether for distance of the observation point from the road, that is much greater than the width of the road, it is necessary to account for single lanes of traffic,

whether one parameter $\varrho = \frac{1}{2}(\varrho_1 + \varrho_2)$ may be considered in the calculations in place of ϱ_1 and ϱ_2.

A positive answer to the second and third questions permits the method to be considerably simplified.

During each measurement leading to the determination of $L_{eq}^{(z)}$, the background level, L_0, was measured, and also the numbers of passing light ($j = 1$) and heavy ($j = 2$) vehicles on both traffic lanes were recorded. (The traffic intensity n_{jk} was calculated). Having also the numerical values of parameters a_{jk}, ϱ_{jk} and V_{jk} from Table 1, the values of L_{eq}, corresponding to the measured values of $L_{eq}^{(z)}$, were calculated from formula (6). The results are shown in Fig. 3.

Table 1. Coefficients a_{jk}, ϱ_{jk} ($j = 1, 2$; $k = 1, 2$) calculated by the linear regression analysis (formula (4))

Vehicle type (j)	Traffic lane (k)	Mean velocity V_{jk} [km/h]	a_{jk}	ϱ_{jk}	Correlation coefficient
light $j = 1$	$k = 1$	65	95.33	2.10	0.941
heavy $j = 2$	$k = 1$	55	103.04	2.12	0.925
light $j = 1$	$k = 2$	65	107.91	2.68	0.885
heavy $j = 2$	$k = 2$	55	117.57	2.89	0.908

Table 2. Coefficients a_j, ϱ_j ($j = 1, 2$) calculated by the linear regression analysis formula 4

Vehicle type (j)	Mean velocity V_j [km/h]	a_j	ϱ_j	Correlation coefficient
light $j = 1$	65	103.09	2.48	0.910
heavy $j = 2$	55	112.48	2.63	0.907

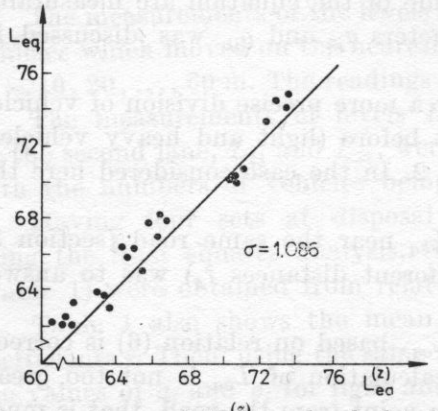

Fig. 3. Measured ($L_{eq}^{(z)}$) and calculated (L_{eq}) values of the equivalent level for the same traffic intensities (calculated according to formula (6))

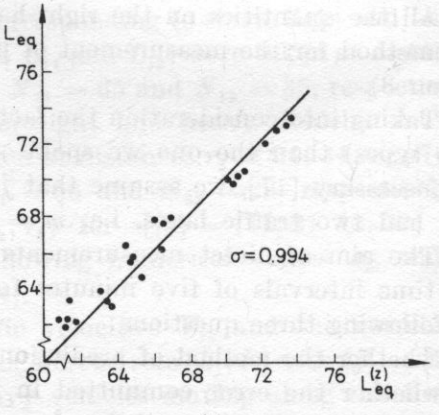

Fig. 4. Measured $L_{eq}^{(z)}$ and calculated (L_{eq}) values of the equivalent level for the same traffic intensities (calculated according to formula (7))

If we assume that all the vehicles move along one path at a distance R from the observation point, then formula (6) takes the form

$$L_{eq} = 10 \log \sqrt{\pi} \left\{ \frac{\Gamma(\frac{1}{2}\varrho_1 - \frac{1}{2})}{\Gamma(\frac{1}{2}\varrho_1)} \frac{10^{0.1a_1} n_1}{V_1 R^{\varrho_1 - 1}} + \frac{\Gamma(\frac{1}{2}\varrho_2 - \frac{1}{2})}{\Gamma(\frac{1}{2}\varrho_2)} \frac{10^{0.1a_2} n_2}{V_2 R^{\varrho_2 - 1}} + 10^{0.1\bar{L}_{eq}} \right\}, \quad (7)$$

where n_1 and n_2 are the intensity of the traffic of light and heavy vehicles on all traffic lanes, V_1, V_2 – traffic velocities of light and heavy vehicles, a_1 a_2, ϱ_1, ϱ_2 – parameters describing light and heavy vehicles as noise sources and the process of the propagation of acoustic wave (section 3), R – a distance from the observation point to the middle of the road (Fig. 2), $\bar{L}_{eq}$ – the equivalent level of the background $\Gamma(x)$ – the Γamma function, respectively.

Inserting into relation (7) the values from Table 2 of a_1, a_2, ϱ_1, ϱ_2 V_1 and V_2, as determined from the measurements of $L_{eq}^{(z)}$, the traffic intensities $n_1 = n_{11} + n_{12}$ and $n_2 = n_{21} + n_{22}$, and distances of measurement points from the middle of the road $R(R = r_1 + 7$ m or $R = r_2 - 7$ m), the values of L_{eq}, shown in Fig. 4, were obtained.

From comparison of the results shown in Figs. 3 and 4, where the values of standard deviations were plotted,

$$\sigma = \left\{ \frac{1}{n} \sum_{i=1}^{n} (L_{eq,i} - L_{eq,i}^{(z)})^2 \right\}^{1/2},$$

it may be seen that using the method based on relation (7), where the traffic lanes are not considered, involves the error of about 1 dB.

The calculations of L_{eq} were performed (on the basis of relation (7)), under the assumption that the equivalent background level $\bar{L}_{eq} = 0$.

For traffic intensities of the order of several hundred vehicles per hour, this assumption is permissible, since the error involved is smaller than 0.1 dB.

With a view to a maximum simplification of the method of prediction of L_{eq}, it was assumed for further calculations that

$$\varrho = \tfrac{1}{2}(\varrho_1 + \varrho_2), \qquad V = \tfrac{1}{2}(V_1 + V_2),$$

hence expression (7) can be rewritten in the following form:

$$L_{eq} = 10 \log \left\{ \sqrt{\pi} \frac{\Gamma(\frac{1}{2}\varrho - \frac{1}{2})}{\Gamma(\frac{1}{2}\varrho)} \frac{(n_1 10^{0.1a_1} + n_2 10^{0.1a_2})}{V R^{\varrho - 1}} \right\}. \quad (8)$$

The results of the calculations of L_{eq} according to this formula are shown in Fig. 5.

The standard deviation σ is in this case of the same order as in Fig. 4, which leads to the conclusion that simplified formula (8) permits L_{eq} to be determined with sufficient exactness. In the formula n_1 and n_2 is traffic intensity of light and heavy vehicles, [veh./hour], $V = \frac{1}{2}(V_1 + V_2)$ – the mean

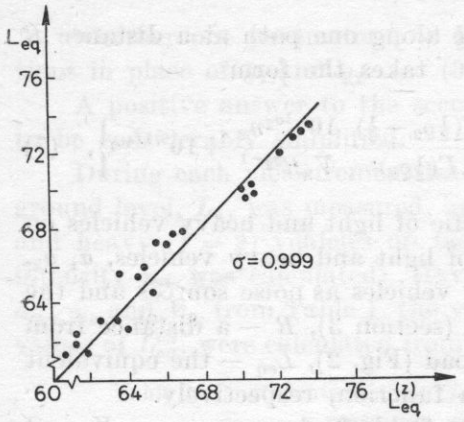

Fig. 5. Measured ($L_{eq}^{(z)}$) and calculated (L_{eq}) values of the equivalent level for the same traffic intensities calculated according to formula (8)

traffic velocity of vehicles of both types [m/h], $\varrho = \frac{1}{2}(\varrho_1 + \varrho_2)$ — the mean value of parameters ϱ_1 and ϱ_2 determined for light and heavy vehicles by the method discussed in section 3, a_1, a_2 — the values of parameter a for light and heavy vehicles, R — a distance from the observation point to the middle of the road.

The investigations showed that a_1, a_2 and ϱ depend on the weather. For example, the investigations performed in winter, near the same road as in section 3, showed that $a_1 = 108.00$, $a_2 = 121.21$, and $\varrho = 2.73$. The measurements being performed at present aim at determination of the values of a_1, a_2, and ϱ for typical weather conditions.

At the same time, the experimental investigations performed near forest roads yielded still other values of these parameters. Plans foresee the broadening of the investigation of parameters a_1, a_2, and ϱ, for differently used areas (parking-lots, greens etc.)

The results obtained from these investigations will permit the present method (formula (8)) to be used in planning on a broader scale.

5. Conclusions

The results from the experimental investigations (Figs. 3, 4, and 5) show that the present methods for determination of the equivalent level near roads with freely flowing traffic (formulae (6), (7) and (8)) are correct, since the standard deviations σ (errors committed when the methods are used) are about 1 dB. The simplest method is particularly correct (σ for this case, Fig. 5, is nearly the same as for more complicated methods, Figs. 3 and 4), which requires consideration of smallest number of parameters (formula (8)) is less complicated, compared to formulae (6) and (7).

The method suggested (section 4) was verified for time periods of several minutes. This, however, does not mean that this method cannot be used for

time intervals of the order of hours, i.e. for arbitrary time of day or night. In this case the mean values of intensities (n_1, n_2) and traffic velocities (V) for these time intervals (e.g. the mean n_1, n_2, V for 8 hours) should be inserted into the relations given above. In this case, however, we must take into consideration the adequate equivalent level of the background, $\bar{L}_{eq}$, variable in 24 hours.

It follows from formula (8) that L_{eq} in the area near the road (Fig. 6) depends on the distance, R, on the parameters describing the traffic, n_1, n_2, V, and the parameters depending on the properties (type of area) of the adjacent area $\{a_1, a_2, \varrho\}$.

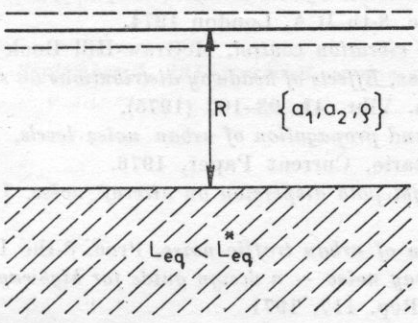

Fig. 6. Location of the area where the equivalent level must not exceed the value L^*_{eq}

The starting point for the establishing of the correctness criteria in planning is the establishment of the value L^*_{eq} which must not be exceeded in the area meant for specific purposes.

It is possible to obtain the inequality $L_{eq} < L^*_{eq}$ in the area considered (Fig. 6) by adequate location of the road with respect to the area (or the area with respect to the road), $R = ?$, if the parameters $\{n_1, n_2, V\}$ and $\{a_1, a_2, \varrho\}$ are known. It follows from equation (8) that $L_{eq} < L^*_{eq}$ if the border of the area is a streight line distant from the middle of the road by

$$R > \left\{ \frac{\sqrt{\pi}\,\Gamma(\frac{1}{2}\varrho - \frac{1}{2})}{\Gamma(\frac{1}{2}\varrho)} \, \frac{n_1 10^{0.1a_1} + n_2 10^{0.1a_2}}{V \cdot 10^{0.1 L^*_{eq}}} \right\}^{1/(\varrho-1)} . \tag{9}$$

Example. Llet us assume that $L^*_{eq} = 60$ dB, $n_1 = 800$ veh./h, $n_2 = 100$ veh./h, and the values of parameters a_1, a_2, $V = \frac{1}{2}(V_1 + V_2)$, $\varrho = \frac{1}{2}(\varrho_1 + \varrho_2)$ are the same as in Table 2. After insertion into (9) we obtain $R > 95$ m, which is the minimum distance from the road of the area where $L_{eq} < 60$ dB.

From the inequality $L_{eq} < L^*_{eq}$ (where L_{eq} is determined by the right-hand side of equation (8)) information can be obtained on the values of parameters $\{n_1, n_2, V\}$, which define the class of the road planned (or the way in which the traffic on the already existent road must be controlled). On the basis of

calculated values $\{a_1, a_2, \varrho\}$ it also gives information how to utilize the area adjacent to the road, to plant gross or trees etc.

In this case a "catalogue of parameters $\{a_1, a_2, \varrho\}$ (determined by the method presented in section 3) for differently covered areas, for different weather conditions, and for different traffic velocities, is necessary.

The authors wish to thank Prof. Dr. hab. Halina RYFFERT, the head of the Institute of Acoustics, for her helpful remarks.

References

[1] G. ANDERSON, *The Transportation System Center* (TSC) *traffic noise prediction model as an experimental tool*, Proc. 8-th ICA, London 1974.

[2] L. L. BERANEK, *Noise and vibration control*, McGraw-Hill Book Camp., N. Y. 1971.

[3] D. E. BLUMENFELD, G. WEISS, *Effects of headway distributions on second order properties of traffic noise*, J. Sound a. Vibr. **41**, 93–102 (1975).

[4] J. S. BRADLEY, *Prediction and propagation of urban noise levels*, Faculty of Eng. Sc. University of Western Ontario, Current Paper, 1976.

[5] L. T. FILOTAS, *Effect of flight path dispersion on aircraft noise*, J. Sound a. Vibr., **48**, 451–460 (1976).

[6] D. J. FISK et al., *Prediction of urban traffic noise*, Proc. 8-the ICA, London 1974.

[7] C. G. GORDON et al., *Highway noise — a design guide for highway engineers*, Cooperat. Nat. Highway Res. Prog. Rep. 117, 1971.

[8] D. R. JOHNSON, E. G. SAUNDERS, *The evaluation of noise from freely flowing road traffic*, J. Sound a. Vibr., **7**, 287–309 (1968).

[9] K. KUNE, K. IKEGAYA, *A statistical investigation on acoustic power radiated by a flow of random point sources*, J. Acoust. Soc. of Japan, **29**, 662–671 (1973).

[10] U. J. KURZE, *Statistics of road traffic noise*, J. Sound a. Vibr., **18**, 171–195 (1971).

[11] H. KUTTRUFF, *Zur Berechnung von Pegelmittelwerten und Schwankungsgrossen bei Strassenlarm*, Acustica, 32, 57–70 (1975).

[12] F. J. LANGDON, *Noise nuisance caused by road traffic in residential areas*, J. Sound a. Vibr., **47**, 246–282 (1976).

[13] S. LJUNGGREN, *A design guide for road traffic noise*, Nat. Swed. Build. Res., D.10 (1973).

[14] R. MAKAREWICZ, *Time-average intensity of sound field generated by moving sources*, Acoustics Letters, **1**, 133–138 (1978).

[15] R. MAKAREWICZ, *A method for determining equivalent level*, Archives of Acoustics, **2**, 83–94 (1977).

[16] R. MAKAREWICZ, *Intensity of sound field generated by a moving source in the semispace with the strafified medium*, Acustica, **44**, 1980 (in press).

[17] R. MAKAREWICZ, G. KERBER, *Method of predicting equivalent level in urban areas*, Archives of Acoustics, **3**, 231–248 (1978).

[18] A. H. MARCUS, *Theoretical prediction of highway noise fluctuations*, JASA, **56**, 132–136 (1974).

[19] M. OHTA, et al., *A statistical theory for road traffic noise based on the composition of co mponent response.*, J. Sound a. Vibr., **52**, 587–601 (1977).

[20] K. S. PEARSON, R. L. BENNETT, *Handbook of noise ratings*, NASA, CR-2376 (1974).

[21] K. J. PLOTKIN, *A case for simple highway noise models*, Wyle Lab., S. C. 50.50, Arlington, 1976.

[22] E. J. RATHE, *Note on two common problems of sound propagation*. J. Sound a. Vibr., **10**, 472–479 (1969).

[23] J. SADOWSKI, B. SZUDROWICZ, *Influence of materials and structures on the acoustic climate in apartments and its effect on the inhabitants health* [*in Polish*], Prace Inst. Techn. Bud., Warszawa 1975.

[24] L. SCHREIBER, *Zur Berechnung des energie-equivalent Dauerschallpegel der Verkehrsgerausche von einer Strasse*, Acustica, **21**, 121–123 (1969).

[25] K. TAKOGI et. al., *Investigations on road traffic noise based on an exponentially distributed vehicles model...*, J. Sound a. Vibr., **36**, 417–431 (1974).

[26] ULLRICH, *Der Einfluss von Fahrzeuggeschwindigkeit und Strassenlag auf den energiequivalent dauerschallpegel*, Acustica, **30**, 90–99 (1974).

[27] K. W. YEOW et al., *Method of predicting L_{eq} created by urban traffic*, J. Sound a. Vibr., **53**, 103–109 (1977).

[28] G. H. WEISS, *On the noise generated by a stream of vehicles*, Transpor. Res., **4**, 229–233 (1970).

Received on September 4, 1978; revised version on January 7, 1979.

ARCHIVES OF ACOUSTICS
5, 2, 169-180 (1980)

THE USE OF AN IMAGE ANALYSER FOR DIMENSIONAL QUANTIFICATION IN ULTRASONIC IMAGES

ROBERT C. CHIVERS

Physics Department, University of Surrey, Guildford, Surrey, UK

HENRY J. W. DUDLEY

Microbiology Department, University of Surrey, Guildford, Surrey, UK.

The use of a sophisticated commercially available image analyser is described in the context of obtaining numerical geometrical data from ultrasonic visualization systems. As an example of its value, its application to the ultrasonic foetal monitoring is discussed. The main features are light pen selection, with immediate display and numerical analysis. Whereas the instrument is too sophisticated for routine use it could be invaluable in ascertaining the design specification of a simpler purpose-built system for incorporation into ultrasonic visualization equipment.

Introduction

Interest in the accurate measurement of the linear dimensions, cross-sectional areas, and volumes of discrete structures within optically opaque media has been growing in recent years in the field of ultrasonic diagnostics, particularly in medical applications.

Linear measurements is usually achieved by employing the pulse-echo technique of the *A*-scan used in sonar, non-destructive testing and medical diagnosis. The time interval between echoes returned from known features of the object is converted, assuming that the velocity of sound in the medium is known, into a measurement of their spatial separation. Alternatively it is possible to take a measurement off a two-dimensional visualization produced, for example, by pulse-echo *B*-scanning [1], *C*-scanning [2], or holography [3], etc. This method still assumes a known velocity of sound in the medium but because of the difficulties of defining exactly the correct plane and the degradation of the information in the *B*-scan (i.e. demodulation, filtering) during

the visualization process, it is generally considered [1], most accurate for the measurement to be made from an *A*-scan trace. The correct *A*-scan direction is chosen with the aid of an associated two-dimensional *B*-scan display.

This technique is only feasible where the structure whose linear dimension is to be measured has a fairly well defined geometry and has good echo-producing extremities. Examples of situations suitable for this type of measurement are foetal biparietal diameter [4], intra-ocular distances [5], and the depth of cracks in metal components [6].

However, when the structure whose linear dimension is to be assessed does not have well defined boundaries (ultrasonically), e.g. a first trimester foetus or a cloud of inclusions in a metal casting, then it is necessary to take the measurement from the two-dimensional (sectional) pictorial display. In addition, measurements such as the perimeter or area of an internal structure have to be taken by hand from the pictorial display, using a map-measurer or a planimeter.

This communication describes the use of a sophisticated image analyser, generally used for the analysis of microscopic images, in this context. Its potential as a useful research tool for defining optimum procedures is discussed, and the possibility of building a much simpler but more specific instrument for use in ultrasonic diagnostics identified.

In the discussion which follows, the medical problem of the assessment of foetal maturity has been chosen as an example of a fairly complex problem in which the analyser may be of considerable value. It is hoped that the parallels with the other areas of ultrasonic materials investigation will be sufficiently clear that specific mention of them would be superfluous.

Analyser

The analyser used for these trials was a commercially available machine, Quantimet 720 *M*, manufactured by Cambridge Scientific Instruments, Royston, Herts, England. It consists essentially [7] of a closed circuit television camera connected to a 720-line non-interlaced display. The video signal is digitised into 8 bits and fed into a memory column by column, storing a total of 604,000 points for the whole screen, with 6 bits of grey scale on each. The input to the analyser may be any optical image, a positive or negative print or transparency. The image processing that can be achieved is extremely varied and flexible, (largely due to the modular construction of the analyser) and includes compensation for uneven illumination. However for the problems reported here, which are of the simplest in image analysis, the most useful facility is the use of a light pen for editing the image displayed on the TV monitor or for selecting a particular region for analysis.

Figure 1 (*a* —*e*) indicates a typical analysis procedure that may be used.

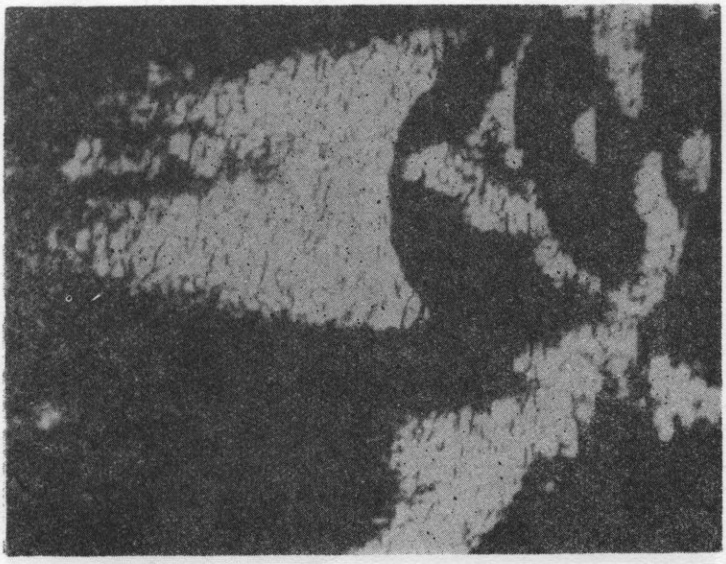

Fig. 1a

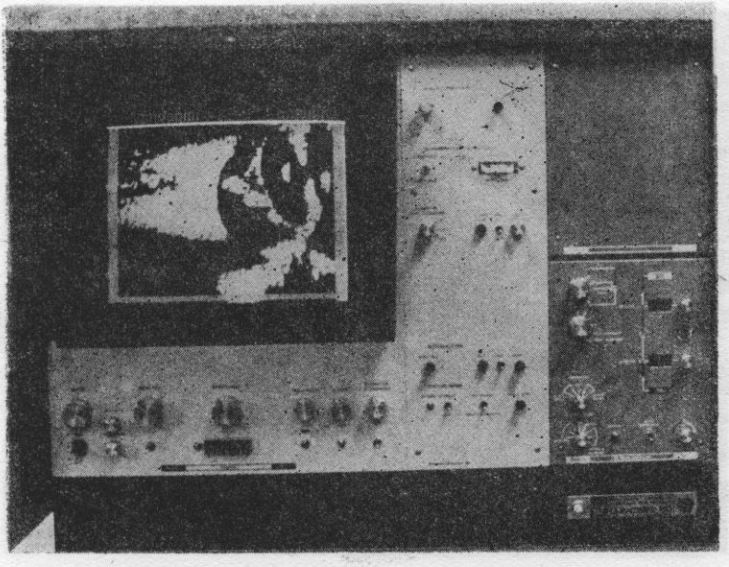

Fig. 1b

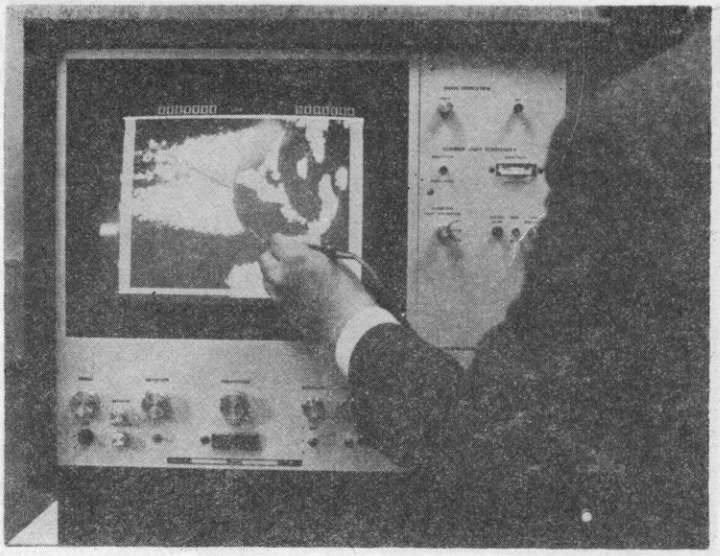

Fig. 1c

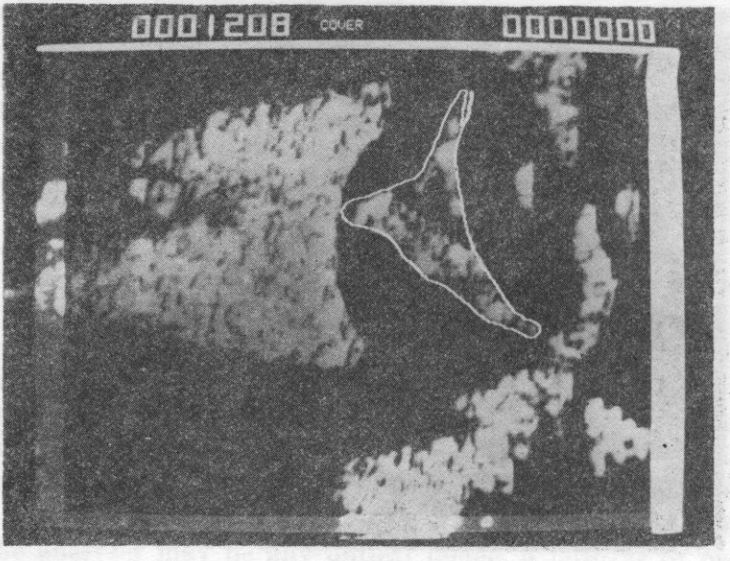

Fig. 1d

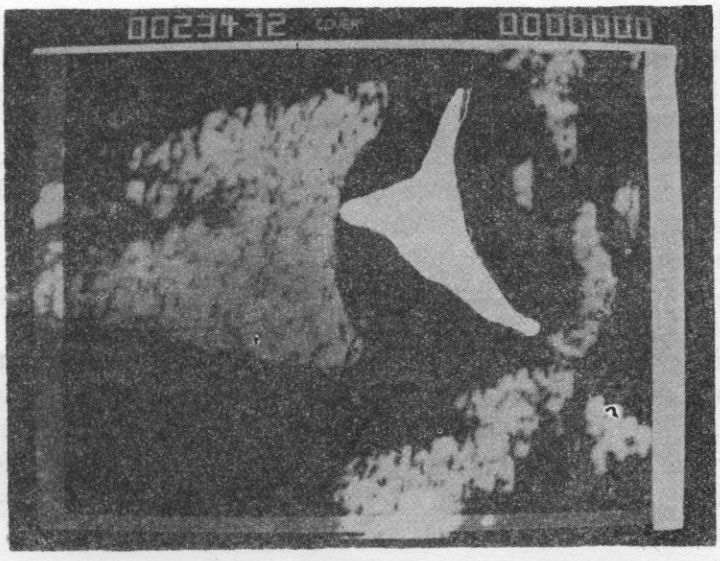

Fig. 1e

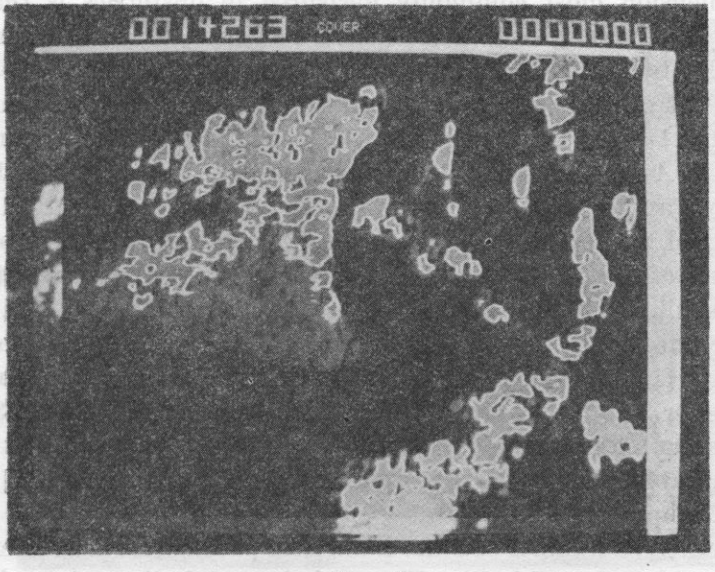

Fig. 1f

Fig. 1. Use of the analyser
a) original image from ultrasonic scanner
b) image displayed on analyser
c) use of the light pen to define an area of interest
d) area displayed and quantified
e) perimeter displayed and quantified
f) typical processed image

Figure 1*a* shows a print from a roll-film negative taken of the display of the ultrasonic scanner. Figure 1*b* shows this picture displayed on the monitor of the analyser. Identification of an area of interest is performed by enscribing it with the light pen (Figure 1*c*). Almost immediately the analyser can display the area enclosed (Figure 1*d*), the perimeter (Figure 1*e*) and in some cases the longest dimension of the area. On the particular simple model available to the present authors, this last measurement was not always easy to achieve although modules are available which would make it comparatively easy. The image processing available may permit the display to be optimised for a particular measurement (Figure 1*f*).

The number at the left at the top of each picture represents the number of picture points. In order to convert it to geometrical area it is necessary to know the scale of the original picture, and to include a scale in the analyser field of view (see Figure 1*d*). The minimum area that may be considered is four picture points.

Application in obstetrics

The dimension most commonly measured in obstetrics is the biparietal diameter of the foetus measured in utero. The usefulness of this measurement was first indicated by DONALD and his colleagues [4, 8], was widely accepted [5, 10], and put on a secure basis by CAMPBELL [11, 12]. Although techniques using only the *A*-scan [10, 13] or only the *B*-scan [14, 15] have been described, the combined *A*- and *B*-scan technique mentioned above, which was first developed by Campbell [11] and has been much adapted [16, 17, 18], is generally considered to be the most accurate for measurement of biparietal diameter, because of the good definition of the echo producing extremities on each side of the skull.

This measurement is, however, only useful for foeti of 14 or more week's gestational age [19], and there has been considerable discussion of the precision, sources of error and accuracy of the technique [10, 16, 20–23, 37] as well of the fundamental methodology employed [24]. It appears that the major sources of variability lie in the definition of the normal curve [24] and in the scanning technique used [25].

More recently, a number of other numerical parameters have been suggested for monitoring foetal well-being. The cephalocaudal dimension of the foetal sac [26], the average diameter of the foetal sac [38], the volume of the foetal sac [27] and the crown-rump length of the foetus [28, 29] have all been suggested as indicators of the gestational age of the foetus during the first 13 weeks. Only the last-named publication gives some indication of the reproducibility of the method.

GARRETT and ROBINSON [15] give curves linking foetal trunk area, occipito-

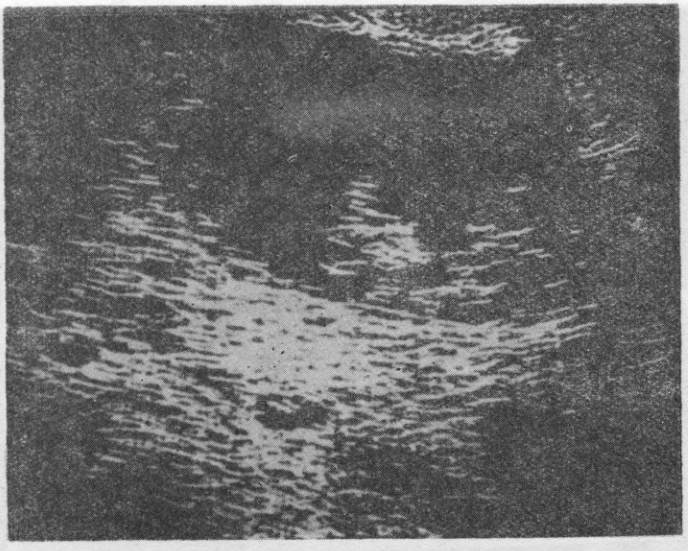

Fig. 2a

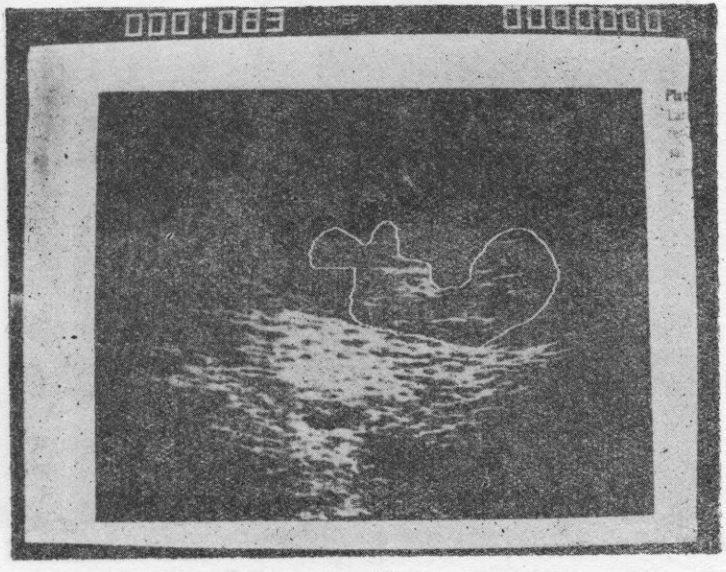

Fig. 2b

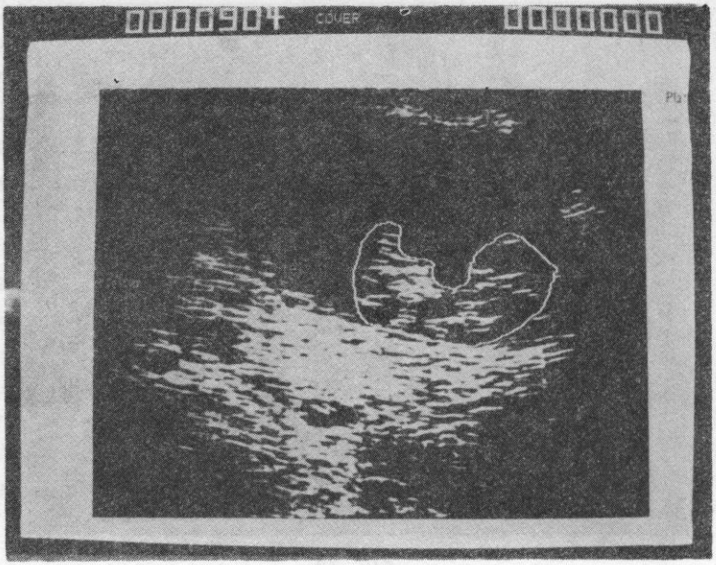

Fig. 2c

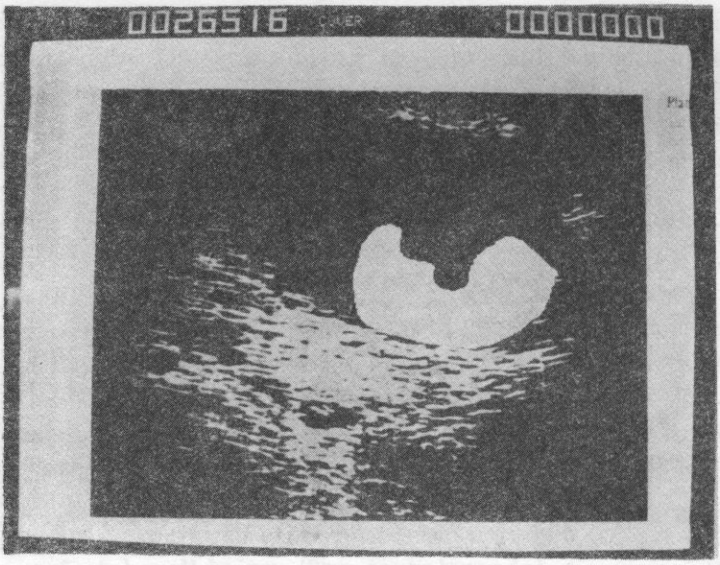

Fig. 2d

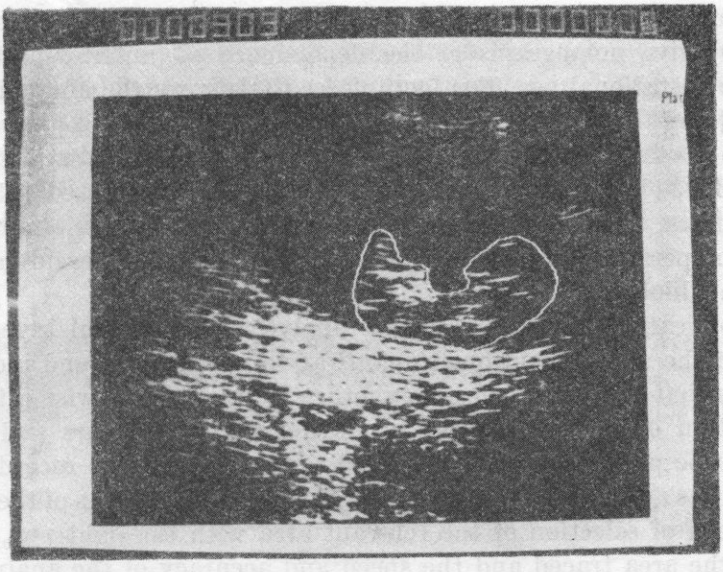

Fig. 2e

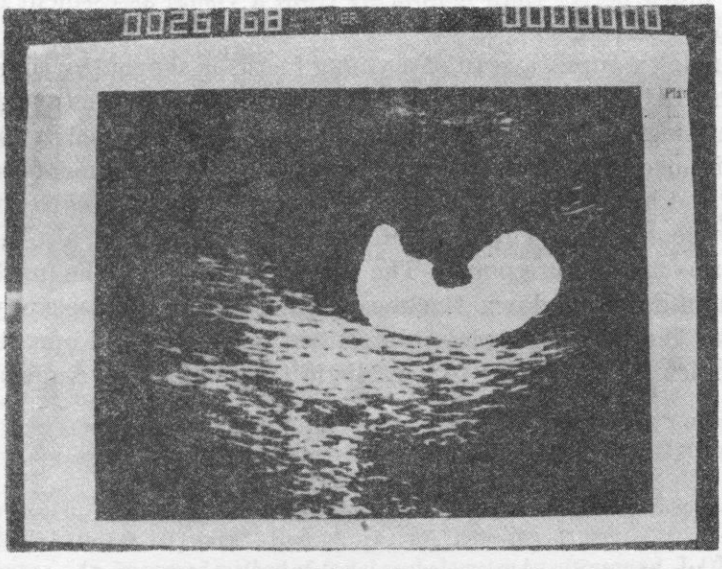

Fig. 2f

Fig. 2. Application of the analyser to foetal assessment
a) original from ultrasonic scanner (courtesy Mrs. R. M. Lunt and Cambridge University Press)
b) selectionont area of interest (erroneous)
c) selection of area of iureerest (preferred) and measured perimeter
d) m afment of corresponding area
e) selectiousand perimeter measurement repeated
e)ɟassociated area measured

frontal diameter and head area to gestational age, while THOMPSON and MAKOWSKI [30] give nomograms of the dependence of anterior-posterior chest diameter on gestational age. For foeti closer to delivery the abdominal circumference [31] and the product of the skull and thorax areas [32] have been used to estimate foetal weight, studies of bladder volume and urine production described [33, 34], and ultrasonic cephalo-pelvimetry proposed [35]. In most of these studies, there is little critical discussion of the variations that may occur due to operator error, the essential limitations of the measurement technique and the biological variations.

The application of the Quantimet analyser to a careful investigation of the value of the above mentioned quantitative parameters (and indeed to any further ones that may be suggested whether foetal or otherwise [19]), is clear. The extraction of numerical data in the form of perimeters and areas, has otherwise to be performed manually, and there is usually no record of the line or area that has actually been considered. The main advantages of the Quantimet are: the speed of selection of the relevant area with the light pen, the identification of the area traced and the speed and accuracy of the analysis. As one of the foremost image analysers available, the quality of the analysis is very high, being much better than it appears from a visual assessment of the image on the display screen.

As a single example, a scan of a young foetus is shown (by courtesy of Mrs. R. M. LUNT [19]) in Figure 2*a*. Outlining the area of the foetus with the light pen can be checked (Figure 2*b*) and may not be considered to be optimum. It may be immediately retraced and checked, the measurements of perimeter (Figure 2*c*) and area (Figure 2*d*) taken, and repeated (Figures 2*e* and 2*f*), with surprisingly good agreement. The crown-rump length was also measured by the analyser as 246 picture points. The whole process, with the machine already set up, including writing down the measurements and photography took only 3–4 minutes. The value of such equipment in the training of operators is considerable, particularly if linked to a realistic tissue model of known dimensions [36].

Conclusion

The application of a commercially available image analyser to the problems of geometrical quantification in ultrasonic visualization in any field has been identified with consideration of the particularly difficult questions raised in medical applications. Particular features of the analyser that are advantageous are the use of a light pen for defining an area of interest, the visualization of the area described and an extremely rapid analysis to give a number of numerical indices, with considerable display flexibility. The quality of the analysis and the flexibility of the analyser in its present form are undoubtedly too sophis-

ticated to be cost-effective in routine use. Nevertheless the analyser may be used to advantage in optimising the procedures that are most useful both in terms of clinical value and operator training in order to define a purpose built system incorporating a light pen and a microprocessor that may be accommodated in commercially available ultrasonic visualization systems where geometrical quantification is important. Detailed studies of specific problems and applications to tissue characterization are in progress and will be discussed in future reports.

Acknowledgements. The authors are grateful to Mrs. Rosemary LUNT of St. Bartholomew's Hospital and Cambridge University Press, for permission to use Figure 2*a*, and to Professor J. E. SMITH of the Microbiology Department for his interest and encouragement.

References

[1] P. N. T. WELLS, *Biomedical Ultrasonics*, Academic Press, New York 1977.

[2] J. MILAN, *An improved ultrasonic scanning system employing a small computer*, Brit. J. Radiol., **45**, 911–916 (1972).

[3] R. C. CHIVERS, *Ultrasonic holography in ophthalmology — physical considerations*, Arch. Acoust., **1**, 51–63, (In Polish: Arch. Ak., **11**, 77–88) (1976).

[4] I. DONALD, T. G. BROWN, *Demonstration of tissue interfaces within the body by ultrasonic echo-sounding*, Brit. J. Radiol., **34**, 539–546 (1961).

[5] J. M. THIJSSEN, *Echo-ophthalmology: physical principles and diagnostic value. In photography, electro-ophthalmology and echo-ophthalmology in ophthalmic diagnosis* (Edited by H. E. HENKES), 271–318, Dr W. Junk by publishers, The Hague, Netherlands, 1973.

[6] J. BLITZ, *Ultrasonics: Methods and Applications*, Butterworths, London 1971.

[7] *The Quantimet in Life Science*, Imanco, Cambridge Instruments, Royston, Herts.

[8] J. WILLOCKS, I. DONALD, T. C. DUGGAN, N. DAY, *Foetal cephalometry by ultrasound*, J. Obstet. Gynaec. Brit. Commonw., **71**, 11–20 (1964).

[9] H. E. THOMPSON, J. H. HOLMES, K. R. GOTTESFELD, E. S. TAYLOR, *Foetal development as determined by ultrasonic pulse-echo techniques*, Am. J. Obstet. Gynaec., **92**, 44–50 (1965).

[10] J. P. DURKAN, G. L. RUSSO, *Ultrasonic foetal cephalometry: accuracy limitations and applications*, Obstet. Gynaec., New York, **27**, 399–403 (1966).

[11] S. CAMPBELL, *An improved method of foetal cephalometry by ultrasound*, J. Obstet. Gynaec. Brit. Commonw., **75**, 568–576.

[12] S. CAMPBELL, G. B. NEWMAN, *Growth of the foetal biparietal diameter during normal pregnancy*, J. Obstet. Gynaec. Brit. Commonw., **78**, 513–519 (1971).

[13] E. I. KOHORN, *An evaluation of ultrasonic foetal cephalometry*, Am. J. Obstet. Gynaec., **97**, 553–559 (1967).

[14] W. N. COHEN, *The prenatal determination of foetal maturity by B-scan ultrasound — comparison with a radiographic method*, Radiology, **103**, 171 (1972).

[15] W. J. GARRETT, D. E. ROBINSON, *Ultrasound in clinical obstetrics*, Charles C. Thomas, Springfield, Illinois, 1970.

[16] R. M. LUNT, T. CHARD, *Reproducibility of measurement of foetal biparietal diameter by ultrasonic cephalometry*, J. Obstet. Gynaec. Brit. Commonw., **81**, 682–685 (1974).
[17] S. CAMPBELL, *Ultrasound in obstetrics*, Brit. J. Hosp. Med., **8**, 541 (1972).
[18] D. WATMOUGH, D. CRIPPIN, J. R. MALLARD, *A modified method of ultrasonic foetal cephalometry*, Brit. J. Radiol., **47**, 352 (1974).
[19] R. M. LUNT, *Handbook of ultrasonic B-scanning in medicine*, Cambridge University Press, Cambridge, England, 1978.
[20] J. M. DAVISON, T. LIND, V. FARR. T. A. WHITTINGHAM, *The limitations of ultrasonic foetal cephalometry*, J. Obstet. Gynaec. Brit. Commonw., **80**, 769–775 (1973).
[21] D. J. WATMOUGH, D. CRIPPEN, J. R. MALLARD, *A critical assesment of ultrasonic foetal cephalometry*, Brit. J. Radiol., **47**, 24–33 (1974).
[22] L. M. HELLMAN, M. KOBAYASHI, L. FILLISTI, M. LAVENMAR, *Sources of error in sonographic foetal mensuration and estimation of growth*, Am. J. Obstet. Gynaec., **99**, 662–670 (1967).
[23] V. POLL, *Ultrasonic cephalometry*, Lancet, **2**, 785 (28 Sept 1974).
[24] R. C. CHIVERS, R. J. PARRY, *Ultrasonic estimation of foetal maturity — a philosophical approach in "Physical Science techniques in obstetrics and gynaecology"*, (Edited by M. M. BLACK and M. E. ENGLISH) 33–40, Pitman Medical, London 1977.
[25] D. WATMOUGH, *Private communication*, 1978.
[26] S. LEVI, F. ERBSMAN, *Croissance du sac embryonnaire humain étudiée par les ultrasons*, Rev. Franc. Gynéc. 69, 3–12 (1974).
[27] H. P. ROBINSON, *'Gestation sac' volumes as determined by sonar in the first trimester of pregnancy*, Brit. J. Obstet. Gynaec, **82**, 100–107 (1975).
[28] H. P. ROBINSON, *Sonar measurement of the foetal crown-rump length as a means of assessing maturity in the first trimester of pregnancy*, Brit. Med. J., **4**, 28–31 (1973).
[29] H. P. ROBINSON, *Ultrasonic application note No. 2*, Nuclear Enterprises Ltd., Edinburgh 1975.
[30] H. E. THOMPSON, E. L. MAKOWSKI, *Estimation of birthweight and gestational age*, Obstet. Gynaec., **37**, 44–47 (1971).
[31] S. CAMPBELL, D. WILKIN, *Ultrasonic measurement of foetal abdominal circumference in the estimation of foetal weight*, Brit. J. Obstet. Gynaec., **82**, 689–697 (1975).
[32] R. LUNT, T. CHARD, *A new method for estimation of foetal weight in late pregnancy by ultrasonic scanning*, Brit. J. Obstet. Gynaec., **83**, 1–5 (1976).
[33] S. CAMPBELL, J. W. WLADIMIROFF, C. J. DEWHURST, *The antinatal measurements of foetal urine production*, J. Obstet. Gynaec. Brit. Commonw., **80**, 680–686 (1973).
[34] J. W. WLADIMIROFF, S. CAMPBELL, *Foetal urine production rates in normal and complicated pregnancy*, Lancet **i**, 151–154 (1974).
[35] A. KRATOCHWIL, N. ZEIBEKIS, *Ultrasonic pelvimetry*, Acta Obstet. Gynaec. Scand., **51**, 357 (1972).
[36] R. C. CHIVERS, R. J. PARRY, *The ultrasonic modelling of human tissue: a prototype foetal head*, in: Proc. Fed. Acoust. Soc. Europe, Warsaw, **2**, (Editors L. LILIPCZYŃSKI and J. K. ZIENIUK) 35–38, PAN, Warsaw 1978.
[37] A. GONZALES, E. DALE, R. BYERS, D. PAGE, *Limitations in prediction of gestational age and birthweight by ultrasonographic methods*, J. Clin. Ultrasound, **6**, 233–238 (1978).
[38] M. BULIC, M. VRTAR, *Ultrasonic planimetry of the gestation sac as a biometric method in early pregnancy*, J. Clin. Ultrasound, **6**, 228–232.

Received on April 20, 1979.

ARCHIVES OF ACOUSTICS
5, 2, 181-188 (1980)

MEASUREMENTS OF PROPAGATION VELOCITY OF ULTRASONIC WAVE AT A FREQUENCY OF 10 MHz IN PURE AND DEUTERATED KDP SINGLE CRYSTALS*

OLGA DELEKTA, ALEKSANDER OPILSKI

Physics Institute, Silesian Technical University (44-100 Gliwice, ul. B. Krzywoustego 2)

The results of determination of all elastic constants of a KH_2PO_4 single crystal (KDP), and in the case of $KD_{2x}H_{2(1-x)}PO_4$ crystals (DKDP) of constants C_{66} i C_{11} and the temperature dependence of the constant C_{66} at a frequency of 10 MHz are reported.

The measurements showed an effect of deuteration on the constant C_{11} and on the change of the temperature dependence of C_{66} in the phase transition region.

1. Introduction

Ferroelectric crystals of the KDP group, both pure and deuterated, are interesting from the point of view of physics, due to the ferroelectric phase transition and the isotopic effect determined by a change of the physical properties of a pure single crystal after introduction of deuterium.

The investigation of dielectric and thermal properties of pure (KDP) and deuterated (DKDP) single crystals has been performed in detail in a wide approach, which is seen in the large number of the reported papers. The elastic properties of these crystals are less often investigated and are usually limited to the pure KDP single crystals or the crystals with special concentration of deuterium [1, 4] and to lower frequencies than those assumed in the overall range of the acoustic investigations in our work.

Information can be obtained from the acoustic investigations, based on the measurements of velocity and attenuation of the elastic wave, related to the static properties and the dynamics of the order parameter which describes the degree of order in a ferroelectric. The use of the acoustic methods for the investigation of ferroelectric phase transitions [8, 10] is particularly recom-

* Work supported by MR. I. 24.

mended when there is disagreement among data on the type of phase transition in the ferroelectric crystal, obtained on the basis of other independent investigations. They can be used in correlation with other experiments to verify the existent theoretical models of the mechanisms of phase transitions [8].

The purpose of this work is the use of the pulse-echo ultrasonic method to investigate the phase transitions in partially deuterated samples of DKDP crystals as a function of deuterium concentration and the frequencies of acoustic waves. The higher frequencies will be used in our further investigations.

The external elastic strain by the order process affects the order parameter. Strong fluctuations of the order parameter in the vicinity of the phase transition cause an increase in some effects connected with measured quantities, e.g. the ultrasonic wave velocity. A change in the ultrasonic wave propagation velocity is essentially determined by the form of coupling between the strain and the order parameter and thus it expresses the static properties of the order parameter. The type of coupling between these quantities is described by the function $F_c(Q_i, \varepsilon_k)$ which occurs in the expansion of the free-energy density in powers of the order parameter Q_i and the components of the strain tensor ε_k [10]. In the case of the KDP type ferroelectrics a linear coupling occurs between the strain and the order parameter,

$$F_c(Q_i, \varepsilon_k) = \beta_{ij} Q_i \varepsilon_j, \tag{1}$$

where Q_i are components of the order parameter, ε_j are the components of the strain tensor, β_{ij} is the coupling parameter.

2. The acoustic measurements of the KDP single crystals

Crystal KDP is a uniaxial ferroelectric with a phase transition temperature $T_c = 122$ K. It undergoes a ferroelectric phase transition from a tetragonal to an orthorombic structure. The order parameter is a spontaneous polarization P_3 directed along the tetragonal c axis. There is a linear coupling [10] between the spontaneous polarization P_3 and the strain ε_6 of the form

$$F_c(\varepsilon_i, P_k) = h_{36} P_3 \varepsilon_6, \tag{2}$$

where the coupling parameter is a relevant component of the piezoelectric stress constant h_{36} at a constant strain.

Only the shear strains are piezoelectrically coupled to the polarization along the c axis. Therefore, the elastic wave which gives information about the type of the phase transition in a KDP crystal is a transverse ultrasonic wave propagating in the (100) direction with its polarization in the (010) direction or a wave with the polarization in (100) propagating in the (010) direction.

Table 1. The elastic constants C_{ij} of a KDP crystal

C_{11}	C_{33}	C_{44}	C_{66}	C_{12}	C_{13}	
10^9 [Nm^{-2}]						
80	80	12.8	6.1	34	41	W. P. Mason 1946 [7]
71.4	56.2	12.7	6.24	−4.9	12.9	W. I. Price 1950 [7]
71.65	56.40	12.48	6.21	−6.27	14.94	S. Haussühl 1964 [2]
71.57	56.61	12.86	6.23	−4.19	14.35	our measurements

The measurements of the ultrasonic wave propagation at a frequency of 10 MHz were performed by the echo-overlap method [9]. The X cut and Y cut quartz transducers were used for generation and detection of the ultrasonic wave. The method used here permits to measure the elastic constants of crystals with an error of less than 0.5 % and a sensitivity of 0.05 % for relative changes in them. This precision relates to the determination of only these elastic constants which are directly expressed through the mass density and the propagation velocity of a sufficient ultrasonic wave. The uncertainty increases respectively in the case of the elastic constants C_{12} and C_{13}, which are expressed not only by the above mentioned quantities, but also by other elastic constants.

The velocities of transverse and longitudinal ultrasonic waves propagating in the sufficiently oriented samples of a KDP single crystal were measured. The values obtained for the elastic constants of a KDP crystal are shown in Table 1 together with data from paper [3].

3. Measurements of the elastic constants C_{66} and C_{11} of DKDP crystals

Only the measurements of the velocity of transverse and longitudinal ultrasonic waves propagating in the (100) direction were performed and the elastic constants C_{66} and C_{11} measured.

The structure symmetry of the KDP type crystals determines that only the elastic constant C_{66} undergoes an anomalous change in the phase transition. The elastic constant C_{11}, however, seemed interesting because of the hydrogen bonds lying very close in the basal (xy) plane. The proton distribution is symmetrical and alongated along the bonds. Measurements of the velocities of the transverse ultrasonic wave V_{12} and the longitudinal ultrasonic wave V_{11} were carried out for three grown DKDP crystals with a different deuteration degree. The results obtained for the elastic constants C_{66} and C_{11} are shown in Table 2.

It should be noted that we observed a change of the elastic constant C_{11} with increasing deuteration in DKDP crystals. This variation of C_{11} is relatively large and exceeds the experimental error, and the investigations will be complemented when completely deuterated crystals have been grown.

Table 2. Phase transition temperatures, T_c, and the elastic constants C_{66} and C_{11} for KDP crystals with a varying deuterium concentration

Deuterium concentration in KDP crystal [mol %]	Phase transition temperature T_c[K]	C_{66} 10^9[Nm^{-2}]	C_{11} 10^9[Nm^{-2}]
0	122	6.23 ± 0.03	71.6 ± 0.4
41.4	166	6.21 ± 0.03	69.9 ± 0.3
57.3	183	6.23 ± 0.03	69.7 ± 0.3
70.4	197	6.20 ± 0.03	69.3 ± 0.3

In addition, measurements of the temperature dependence of the elastic constant C_{66} for three DKDP crystals with a different degree of deuteration were made. The experimental results for $C_{66}(T)$ are shown in Figs. 1, 2, and 3, respectively.

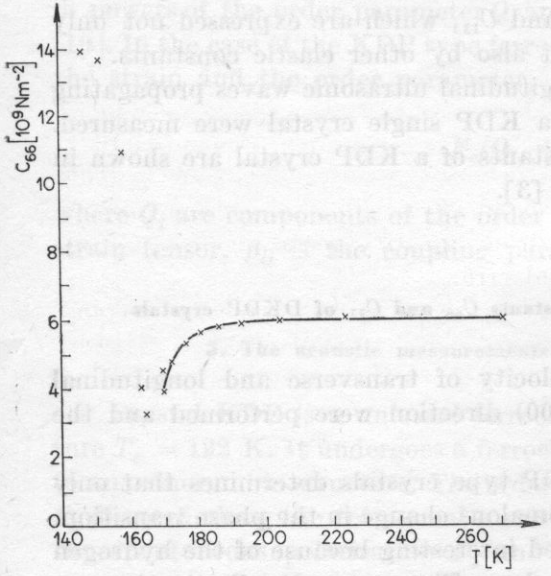

Fig. 1. Temperature dependence of the constant $C_{66}^{E=0}$ for a DKDP crystal with a deuterium concentration of 41.4 mol%

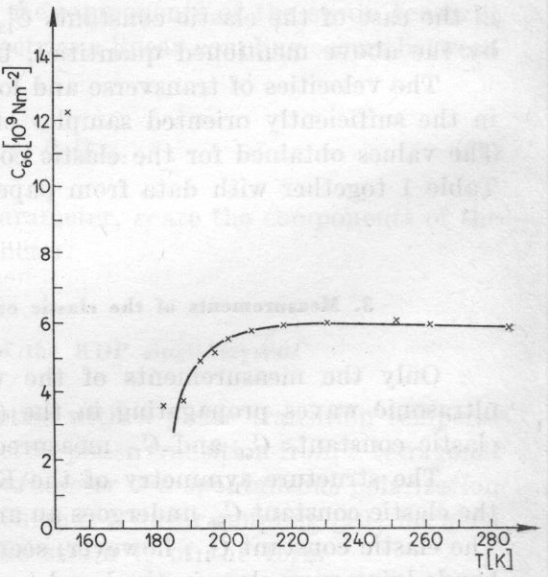

Fig. 2. Temperature dependence of C_{66}^{E} for a DKDP crystal with a deuterium concentration of 57.3 mol%

On the basis of the obtained plots of the dependence $C_{66}(T)$, the values of the phase transition temperatures, T_c, for each DKDP crystal were determined. From the linear dependence of the phase transition temperature T_c on the deuterium concentration in a crystal [5],

$$T_c = 121.7K + 1.07x, \tag{3}$$

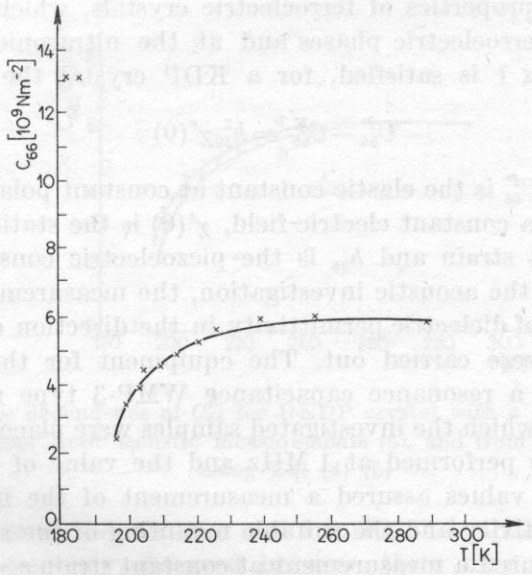

Fig. 3. Temperature dependence of C_{66}^E for a DKDP crystal with a deuterium concentration of 70.4 mol%

the deuteration degree of the crystals investigated was determined. Here x is the deuterium concentration in a DKDP crystal expressed in mol%. The results are given in Table 2. The linear dependence of T_c (x) in the form of (3) is generally used and possible deviations from linearity according to [11] are small and do not exceed the experimental error.

In the first stage of the investigations, despite the use of the method recommended for growing DKDP crystals [2], no completely deuterated crystals were obtained.

4. Discussion of the experimental results

The disagreement occurring among the literature data with respect to the elastic constants C_{ij} of a KDP single crystal [3] required a determination of the elastic constants for the KDP crystals used in the investigations. The values obtained for C_{ij} were determined with an accuracy of more than 0.5%. The values of C_{ij} for KDP, obtained in [3] previously, involve larger errors, and only the measurements of HAUSSÜHL and PRICE and HUNTINGTON [2], which were carried out with a similar accuracy, agree with the authors measurements.

The variation observed for the elastic constant C_{11} with an increasing deuteration in DKDP crystals suggests that the O—H—O bonds will become weaker upon the substitution of D for H. From the relation between the die-

lectric and elastic properties of ferroelectric crystals, which are piezoelectrics in the para- and ferroelectric phases and at the ultrasonic frequency, when the condition $\omega\tau \ll 1$ is satisfied, for a KDP crystal the relation

$$C_{66}^{P} - C_{66}^{E} = h_{36}^{2}\chi^{s}(0) \tag{4}$$

is valid [7], where C_{66}^{P} is the elastic constant at constant polarization, C_{66}^{E} is the elastic constant at a constant electric field, $\chi^{s}(0)$ is the static dielectric susceptibility at constant strain and h_{36} is the piezoelectric constant.

In addition to the acoustic investigation, the measurements of the temperature dependence of dielectric permittivity in the direction of the spontaneous polarization axis were carried out. The equipment for the measurement of $\varepsilon'_{33}(T)$ consisted of a resonance capacitance WMP-3 type meter and a measuring chamber, in which the investigated samples were placed. The capacitance measurements were performed at 1 MHz and the value of measuring voltage was 10 mV. These values assured a measurement of the nearly static value of dielectric permittivity and the suitable mounting of the sample in the measuring chamber assured a measurement at constant strain $s = 0$. Measurements of ε'_{33} were made with an accuracy of about 5 %. Temperature stability during the measurements was ± 0.01 K.

On the basis of measurements of $\varepsilon'_{33}(T)$, the variation in the elastic constant $C_{66}^{E}(T)$, according to Eq. (4), was calculated for a DKDP crystal with the highest deuteration degree ($x = 70.4$ mol %), in order to compare it with an experimentally obtained change in $C_{66}^{E}(T)$. The results obtained are shown in Fig. 4. Relevant values of h_{36} and C_{66}^{P}([5], p. 86 and 107] and of $\varepsilon'_{33}(T)$ and $C_{66}^{E=0}$, which were used in the calculations, are given in Table 3.

Table 3. Temperature dependencies of h_{36}, C_{66}^{P} and ε_{33} used for the calculation of $C_{66}^{E}(T)$ from Eq. (4)

Temperature [K]	h_{36}* 10^{8} [NC^{-1}]	C_{66}^{P}** 10^{9} [Nm^{-2}]	Temperature T [K]	ε_{33}***
373	6.48	5.9	255	80
313	7.05	6.0	238	125
293	7.32		226	184
273	7.50	6.2	220	236
253	7.74		213	303
233	7.98		210	371
213	8.19		205	411
193	8.37	6.5	203	452
173	8.43		199	596
123	9.21	7.0	196	707
			195	702
			193	664
			191	605

*[3], p. 86 **[3], p. 107 ***-our measurements

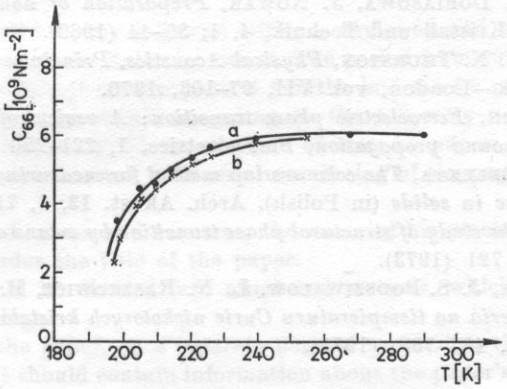

Fig. 4. Temperature dependence of C_{66}^E for DKDP crystal with a deuterium concentration of 70.4 mol% obtained from acoustic measurements (a), and from dielectric measurements using Eq. (4) (b)

The character of the curves *a* and *b* in Fig. 4 is analogous, and the stable quantitative discrepancy observed between them may suggest a systematic error between the experimental data and those calculated from Eq. (4). A source of the error may be the values of C_{66}^P and h_{36}, which were used in the calculations and were not measured for crystals investigated here.

Comparison of curves $C_{66}^E(T)$ from Figs. 1 and 3, obtained for two most differential deuterated samples, does not give an essential change of the character of dependence of $C_{66}(T)$ on increasing deuteration and only a well-known isotope effect on T_c is obtained.

An investigation of elastic constants in the region very close to T_c for DKDP crystals with a varying deuterium concentration seems more interesting on the low-temperature side of T_c, due to the possibility of other isotopic effects occurring and that of observing a possible change of the order phase transition due to deuteration.

References

[1] C. W. Garland, D.B. Novotny, *Ultrasonic velocity and attenuation in KH_2PO_4*, Phys. Rev. **117**, 2, 971–975 (1969).

[2] S. Haussühl, *Elastische und thermoelastische Eigenschaften von KH_2PO_4, KH_2AsO_4, $NH_4H_2PO_4$, $NH_4H_2AsO_4$ und RbH_2PO_4*, Zeit. Kristall. Bd. **120**, 401–414 (1964).

[3] Landolt-Börnstein, *Numerical data and functional relationships in science and technology, Group III: Crystals and solid state physics*, Springer-Verlag, Berlin – Heidelberg 1966.

[4] E. Litov, E. A. Uehling, *Polarization relaxation in the ferroelectric transition region of KD_2PO_4*, Phys. Rev. Letters, **21**, 12, 809–812 (1968).

[5] G. M. Ioiacono, J. S. Balascio, W. Osborne, *Effect of deuteration on the ferroelectric transition temperature and the distribution coefficient of deuterium in $K(H_{1-x}D_x)_2PO_4$*, Appl. Phys. Letters, **24**, 10, 455–456 (1974).

[6] V. Marecek, L. Dobiasowa, J. Nowak, *Preparation of non-wedgeshaped* KDP *and* DKDP *crystals*, Kristall und Technik, **4**, 1, 39–44 (1969).

[7] W. P. Mason, R. N. Thurston, *Physical Acoustics, Principles and Methods*, Academic Press, New York–London, vol. VII, 97–103, 1970.

[8] R. E. Nettleton, *Ferroelectric phase transition: A review of theory and experiment, Part 8 – Ultrasound propagation*, Ferroelectrics, **1**, 221–226 (1970).

[9] A. Opilski, O. Delekta, *The echo overlap method for measuring the propagation velocity of ultrasonic wave in solids* (in Polish), Arch. Akust. **13**, 1, 71–76 (1978).

[10] W. Rehwald, *The study of structural phase transition by means of ultrasonic experiments*, Adv. Phys. **22**, 721 (1973).

[11] E. N. Wołkowa, J. S. Podsziwałow, Ł. N. Raszkowicz, B. A. Strukow, *Wlijanie koncentracji dejtieria na tiempieraturu Curie niekotorych kristałow grupy* KDP, Izwiestia AN SSSR, **39**, 4, 487–790, (1975).

Received on October 12, 1978; revised version on May 25, 1979.